AD-A088 223 NAVAL SURFACE WEAPONS CENTER SILVER SPRING MD F/G 19/1
DETONATIONS AND MOLECULAR ELECTRONIC STRUCTURE OF EXPLOSIVES: T--ETC(U)
MAY 80 R D BARDO
UNCLASSIFIED NSWC/TR-79-175 NL

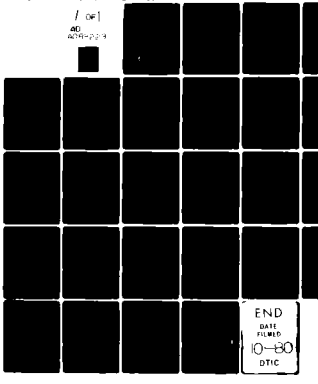

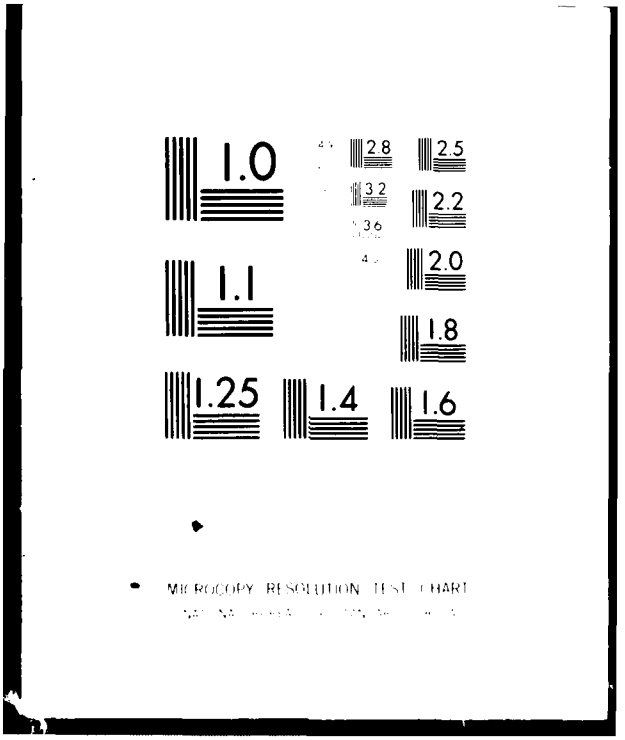
1.0
2.8
2.5
3.2
2.2
3.6
2.0
1.1
1.8
1.25
1.4
1.6
MICROCOPY RESOLUTION TEST CHART

NSWC TR 79-175

DETONATIONS AND MOLECULAR ELECTRONIC STRUCTURE OF EXPLOSIVES: THEORY AND ITS APPLICATION TO $(NO^+)_n$

RICHARD D. BARDO

RESEARCH AND TECHNOLOGY DEPARTMENT

30 MAY 1980

NAVAL SURFACE WEAPONS CENTER

Dahlgren, Virginia 22448 • Silver Spring, Maryland 20910

UNCLASSIFIED

SECURITY CLASSIFICATION OF THIS PAGE (When Data Entered)

REPORT DOCUMENTATION PAGE	READ INSTRUCTIONS BEFORE COMPLETING FORM
1. REPORT NUMBER: NSWC/TR-79-175	2. GOVT ACCESSION NO.: AD-A088223
3. RECIPIENT'S CATALOG NUMBER: (9)	
4. TITLE (and Subtitle): Detonations and Molecular Electronic Structure of Explosives: Theory and Its Application to $(NO^+)_n$.	5. TYPE OF REPORT & PERIOD COVERED: Technical Report - Oct 1977 – Dec 1978
	6. PERFORMING ORG. REPORT NUMBER
7. AUTHOR(s): Richard D. Bardo	8. CONTRACT OR GRANT NUMBER(s)
9. PERFORMING ORGANIZATION NAME AND ADDRESS: Naval Surface Weapons Center, White Oak, Silver Spring, Maryland 20910	10. PROGRAM ELEMENT, PROJECT, TASK AREA & WORK UNIT NUMBERS: Task Number ZR011301, IR-221; Task Number ZR01305, IR-214
11. CONTROLLING OFFICE NAME AND ADDRESS: (12) 57 (11)	12. REPORT DATE: 30 May 1980
	13. NUMBER OF PAGES: 56
14. MONITORING AGENCY NAME & ADDRESS (if different from Controlling Office): (16) ZR01301, ZR01305	15. SECURITY CLASS. (of this report): UNCLASSIFIED
	15a. DECLASSIFICATION/DOWNGRADING SCHEDULE

16. DISTRIBUTION STATEMENT (of this Report)

Approved for public release; distribution unlimited.

17. DISTRIBUTION STATEMENT (of the abstract entered in Block 20, if different from Report)

18. SUPPLEMENTARY NOTES

19. KEY WORDS (Continue on reverse side if necessary and identify by block number)

20. ABSTRACT (Continue on reverse side if necessary and identify by block number)

The theory of the electronic structure of molecular systems is discussed. It is suggested that certain electronic excited states are diminished in energy during compression, and that intersections of ground and excited state potential energy surfaces occur, thereby creating much lower activation energy barriers and greatly enhancing reaction rates. The molecular

DD FORM 1 JAN 73 1473 EDITION OF 1 NOV 65 IS OBSOLETE S/N 0102-LF-014-6601

UNCLASSIFIED

SECURITY CLASSIFICATION OF THIS PAGE (When Data Entered)

411563

system $(NO^+)_n$ is treated here as a prototype explosive system. Ab initio and semiempirical calculations on the ground and excited electronic states of $(NO^+)_n$ are presented. Intersections of the surfaces are seen to occur, suggesting that at high compressions the activation energy for bond scission may be substantially reduced. It is also shown that the changes in excitation energies depend primarily on the interactions of two or three NO^+ molecules, which suggests an enormous simplification in the study of excited states.

FOREWORD

The theory of the electronic structure of molecular systems is discussed. The potential energy surface is described as a conceptual and computational tool in the study of the kinetics of fast reactions which might occur in detonations. It is suggested that certain excited states are diminished in energy during compression, and that intersections of ground and excited state potential energy surfaces occur, thereby creating much lower activation energy barriers and greatly enhancing reaction rates.

Ab initio and semiempirical calculations of ground and excited electronic states are performed on the prototype molecular explosive system, $(NO^+)_n$. Each NO^+ molecule is allowed to interact with the other molecules, as a model of various states of compression. The results of the calculations show that the intersections are forced to occur under compression, and that the activation energy for the N-O bond scission process is substantially reduced from its gaseous state value of 254 kcal/mole. The results also show that IR and UV spectra are shifted to lower frequencies. These calculations are the first in a series to be performed on explosive molecules, from which criteria for sensitivity to shock initiation leading to detonation will be deduced. The author thanks Drs. D. J. Pastine, M. J. Kamlet, E. T. Toton, and S. J. Jacobs for helpful discussions. This work was carried out under Task Number ZR01301, IR-221, and Task Number ZR01305, IR-214.

Elihu Zimet

ELIHU ZIMET
By direction

CONTENTS

ILLUSTRATIONS

INTRODUCTION

The sensitivity of an explosive is often categorized in terms of its response to stimuli such as impact,[1] friction,[2] and shock.[3] In Reference 1, it was demonstrated for a variety of high (secondary) explosives that an impact explosion behaves like a low temperature thermal decomposition which implies that temperature is required for initiation here. In that work, impact sensitivity trends were deduced on the basis of molecular structure. In the case of friction sensitivity,[2] temperature again determines initiation to explosion. As indicated in Reference 3, the critical pressure-time profiles required to achieve a shock transition to detonation are determined by the chemical and physical nature of the explosive as well as the explosive dimensions. Our knowledge of the chemical and physical nature of an explosive derives from theoretical and empirical considerations. In view of the complexity of the response of explosives to the various stimuli, any approach which attempts to relate the totality of the chemical and physical characteristics of an explosive to sensitivity must be semiempirical in nature.

Pressure plays a crucial role in the shock initiation of detonation. The pressure-time profile relationship $P^n t$ = const. has been deduced from a theoretical consideration of relaxation processes which channel energy into an explosive molecule.[4] Here, the pressure P consists of a temperature-dependent term P_T as well as a term arising from molecular interactions at 0°K, $P_0 = -dE/dV$, where E is the internal energy and V is the volume. These contributions to P are well understood when examined from the point of view of an equation of state.[5] On the other hand, the relative importance of these terms is not understood with respect to the shock initiation of detonation problem. It is well known that shock compression produces high temperatures which always accelerate chemical reactions, and which generate the term P_T. For example, a shock wave in liquid

---

[1]Kamlet, M. J., "The Relationship of Impact Sensitivity with Structure of Organic High Explosives. I. Polynitroaliphatic Explosives" in Proceedings of the Sixth Symposium (International) on Detonation, 24 August 1976, pp. 312-322.

[2]Bowden, F. P., and Yoffe, A. D., Initiation and Growth of Explosions in Liquids and Solids, (Cambridge University Press, 1952).

[3]Price, D., "Shock Sensitivity, A Property of Many Aspects," in Proceedings of the Fifth Symposium (International) on Detonation, 18 August 1970, pp. 207-217.

[4]Pastine, D. J., Edwards, D. J., Jones, H. D., Richmond, C. T. and Kim, K., "Some New Concepts Relating to the Initiation and Failure of Detonable Explosives," in Timmerhaus, K. D., and Barber, M. S., eds., High-Pressure Science and technology, Vol. 2, (New York: Plenum Publishing Corp. 1979), pp. 364-382.

[5]Pastine, D. J., and Bernecker, R. R., "P,V,E,T Equation of State for 1,3,5-triamino-2,4,6-trinitrobenzene," Journal of Applied Physics, Vol. 45, No. 10, 1974, p. 4458.

nitromethane produces detonation within a few microseconds when the explosive is compressed to 60% of its original volume and the temperature reaches 1140°K.[6] However, little is currently known about the detailed mechanism which relates P_0 to initiation and to the steady-state propagation. This information is needed for a fundamental understanding of sensitivity to detonation as well as for the correct classification of explosives according to their sensitivity, which is essential for their safety and handling.

The interpretation of the mechanism of initiation requires the consideration of all of the microscopic and macroscopic characteristics of an explosive, the former being the most difficult, if not impossible, to analyze experimentally at high pressures and temperatures.[7] An understanding of the microscopic aspects is of prime importance to the chemist who is confronted with synthesizing explosive molecules. Conditions in the laboratory permit the tailoring of molecules which meet specific requirements for weapons systems. If new insensitive high explosive molecules are to be synthesized, it should be possible to recognize those pertinent intrinsic structural features which define sensitivity, as distinct from those apparent features derived from macroscopic considerations. In this report, a program is introduced, the ultimate objective of which is to define criteria for initiation of detonation and to interpret the steady-state detonation based on the electronic structure of molecules comprising explosives.

Semiempirical computational methods have been used to relate electronic structure and sensitivity.[8] These very approximate calculations dealt with only the ground electronic states. However, a recent series of calculations has been used to determine a striking correlation between sensitivities to detonation and electronic charge distributions in the excited states of the molecules TATB and five other nitroaromatics, tetryl and six other nitroamines, and nitroglycerine and seven other nitric esters.[9] These calculations were performed on the isolated molecules, and did not address the question of whether the energy in the explosive is sufficiently

---

[6]Campbell, A. W., Davis, W. C., and Travis, J. R., "Shock Initiation of Detonation in Liquid Explosives," Physics of Fluids, Vol. 4, No. 4, 1961, p. 498.

[7]Bardo, R. D., Hall, T. N., and Kamlet, M. J., "The Volume of Activation in the Shock Initiation of Explosives," Combustion and Flame, Vol. 35, 1979, p. 259.

[8]Haskins, P. J., "Electronic Structure of Some Explosives and Its Relationship to Sensitivity," Research in Primary Explosives-ERDE 1975, Presentation No. 6, 1975.

[9]Delpuech, A., and Cherville, J., "Relation entre la Structure et la Sensibilité au Choc des Explosifs Secondaires Nitrés-Critére Moléculaire de Sensibilité. I. Cas des Nitroaromatiques et des Nitramines," Propellants and Explosives, Vol. 3, 1978, p. 169.

large and localized to reach excited states. In the present report, we are interested in interacting molecules as a simulation of compressed states, in order to determine trends and changes in the ground and excited electronic states and the corresponding changes in electronic excitation energies. The calculations will require the development of new theory based on the wave equations of Reference 10 and a utilization of both ab initio and semiempirical computational methods.

It will be shown from the methods of quantum mechanics how activation energies are related to electronic structure, and how these energies and the corresponding reaction rates change as the molecular electronic structure is altered under compression. It will be seen that direct excitation of electronic states need not occur for certain excited states to contribute to reaction processes. In the case of interacting NO^+ molecules, a 0^oK isotherm will be presented. The results of preliminary calculations on the NO^+ molecules and the relationship to sensitivity will be discussed.

THE MICROSCOPIC AND MACROSCOPIC ASPECTS OF SENSITIVITY TO DETONATION

A complete analysis of the sensitivity to detonation problem requires a consideration of microscopic and macroscopic characteristics of matter. The microscopic properties are described in terms of molecular electronic structure, motions of nuclei, and the kinds of reactions which can occur. The macroscopic properties are related to the homogeneity and heterogeneity of the explosive, the mechanical response, which includes shear stresses and strains, and explosive dimensionality parameters such as critical diameters which give the minimum charge diameter in which a steady state detonation will propagate.

Considerable progress has been made in determining relationships between sensitivity and the macroscopic aspects. It is generally recognized that homogeneous explosives initiate through a thermal explosion which occurs at the entering face of the acceptor, where the explosive has been heated in its compressed state for the longest period of time. Substantial confirmation of this process has been achieved by Hardesty[11] in a detailed experimental study of liquid nitromethane. Increasing the heterogeneity of an explosive can change its sensitivity.[12] For example, the introduction of argon

---

[10]Bardo, R. D., and Wolfsberg, M., "The Wave Equation of a Nonlinear Triatomic Molecule and the Adiabatic Correction to the Born-Oppenheimer Approximation," Journal of Chemical Physics, Vol. 67 No. 2, 1977, p. 593.

[11]Hardesty, D. R., "An Investigation of the Shock Initiation of Liquid Nitromethane," Combustion and Flame, Vol. 27, 1976, p. 229.

[12]U. S. Army Materiel Command, Engineering Design Handbook, Principles of Explosive Behavior, 1972, Chapter 11, pp. 1-32.

gas into nitromethane creates hot spots at the positions of the bubbles, where local ignitions occur before an entire cross section of nitromethane is ignited.[12] In general, hot spots, which arise as a consequence of shocking, are distinguished as hydrodynamic and temperature and pressure related, and apparently are instrumental in causing heterogeneous explosives to initiate directly behind the shock front, in contrast to the situation found in homogeneous explosives.[12]

Bridgman[13] has demonstrated that shear stresses and strains lead to explosive decomposition of hydrostatically compressed materials. At the present time, it is not known exactly what role strain plays in the initiation of a shocked explosive, although Teller has dealt qualitatively with this problem.[14] The pressures in shocked materials are generally believed to be hydrostatic in nature, since the yield strengths are greatly exceeded. These pressures relate to average distributions of molecules which are achieved on a time scale which may be long compared to times associated with other processes occuring on the microscopic scale.[15]

The characteristic times required to yield commonly observed microscopic and macroscopic effects in matter range from 10^{-16} to 10^{-5} sec. The orbital time for electronic motion is the order of 10^{-16} to 10^{-15} sec. Since nuclei are much more massive than electrons ($m_{nucleus}/m_{electron} > 1800$), the period for optic mode vibrations is generally 10^{-14} to 10^{-13} sec., and the period for acoustic mode vibrations is 10^{-13} to 10^{-12} sec. The times required to attain local and global thermodynamic equilibria in shocked liquids are 10^{-10} sec. and 10^{-7} sec., respectively. The time for nucleation of solid material from the liquid state is greater than the 1-10 μsec. duration in shock compression experiments. On the basis of the above times, then, any molecular model which relates sensitivity to molecular structure must answer the question: why does the initiation process take times in microseconds as compared with the much shorter times for elementary motions within the molecules? Pastine, et al.[4] have addressed this question in terms of molecular relaxation processes. Edward Toton of this Center is using relationships between the rapid electronic motion on the one hand and the much slower nuclear motion on the other to examine the nature of the process which

---

[13]Bridgman, P. W., "Effects of High Shearing Stress Combined with High Hydrostatic Pressure," Physical Review, Vol. 48, 1935, p. 825.

[14]Teller, E., "On the Speed of Reactions at High Pressures," Journal of Chemical Physics, Vol. 36, No. 4, 1962, p. 901.

[15]Johnson, Q., Mitchell, A., Keeler, R. N., and Evans, L., "X-ray Diffraction during Shock Wave Compression," Physical Review Letters, Vol. 25, 1970, p. 1099. In this paper, the results of the X-ray analysis of crystalline LiF demonstrate that the uniaxially strained crystal produced by a 130 kbar shock relaxes to an isotropic structure in a time which is short compared to 20 nanoseconds.

channels energy from the lattice vibrational modes of an explosive into the optic vibrational modes of a given molecule. In the Sections entitled, "The Quantum Mechanical Problem" and "Calculations of Ground and Excited States for the $(NO^+)_n$ Molecular System" of this report, we shall begin to address the above question from the point of view of how the energy within the explosive molecule is utilized to break bonds.

THE ACTIVATION ENERGY AS A POTENTIAL ENERGY CONCEPT

The reaction rate equations of a reacting fluid are given by

$$\frac{dn_j}{dt} = \sum_{i=1}^{r} \Gamma_i a_{ij} \quad , \quad j = 1,2,...N \quad , \qquad (1)$$

where r is the total number of distinct reactions occurring, a_{ij} a positive or negative integer or rational number if substance j^{ij} participates in the reaction i, and $a_{ij} = 0$ if substance j does not participate. Here, Γ_i is a function of the pressure P, temperature T, and N composition variables n_j,

$$\Gamma_i = \Gamma_i(P,T,n_1,n_2,...n_N) \quad , \quad i = 1,2,...r \quad . \qquad (2)$$

Γ_i has the general form

$$\Gamma_i = k_i F_i \quad , \qquad (3)$$

where k_i is the rate coefficient for the i-th reaction and is a function of P and T, anf F_i is a function of the composition variables. The mathematical form of F_i contains products of the composition variables. On the other hand, k_i describes the nature of the reaction taking place and utilizes information pertaining to molecular structure and the probabilities of intramolecular and intermolecular energy transfer. Since molecular structure and the probabilities depend on P and T, the fundamental parameters contained in k_i of Equation (3) and the mathematical form of k_i will also vary with P and T.

When P and T vary simultaneously, the variation of $\ln k_i$ with $1/T$ is[7]

$$\frac{d\ln k_i}{d(1/T)} = -\frac{E_{act,i}}{R} + \frac{TV_{act,i}}{R}\frac{dP}{dT} \quad , \qquad (4)$$

where R is the gas constant and*

$$E_{act,i}(P,T) = -R\left(\frac{\partial \ln k_i}{\partial (1/T)}\right)_P \qquad (5)$$

and

$$V_{act,i}(P,T) = RT\left(\frac{\partial \ln k_i}{\partial P}\right)_T \quad . \qquad (6)$$

The quantities $E_{act,i}$ and $V_{act,i}$ are the energy of activation and the volume of activation, respectively, for the i-th reaction. They are intimately related to molecular structure.**

The analysis in Reference (7) demonstrates that the function

$$E^{int}_{act,i} = E_{act,i} - PV_{act,i} \qquad (7)$$

is an internal energy of activation. It is this quantity which is closely related to the changes in potential energy when the reactants pass from their ground states to the activated state in the i-th reaction.***

Integration of Equation (4) reveals that k_i in Equation (3) contains $\exp(-E_{act,i}/RT)$, which is the probability that the reacting system has an energy of $E^{int}_{act,i}$ or greater. One may then speak of the reacting system as having surmounted a barrier $E^{int}_{act,i}$ in height. This activation barrier is imbedded in a potential energy hypersurface of dimensionality given by the geometrical degrees of freedom of the reacting system. The hypersurface has its origin in the quantum mechanical description of the reacting system. Such a description constitutes the most fundamental analysis for the system. A discussion of the utility of the potential energy hypersurface in

---

*The variables V and T may also be chosen. The variables P and T have been selected here since V_{act} is widely used by chemists to interpret reaction mechanisms.

**Since E_{act} is defined by the partial derivative in Equation (5), it is not what one would call the Arrhenius activation energy, which is defined by the total derivative in Equation (4).

***It is noted here that if $P = cT$ (c not a function of T) is substituted into Equation (4), E^{int}_{act} becomes an Arrhenius activation energy. However, $P = P_0 + P_T$, so that, in general, $P = cT$ will not be an adequate approximation.

chemical kinetics is given by Laidler.[16]* A detailed discussion of these hypersurfaces is presented in the Section entitled, "The Quantum Mechanical Problem."

THE QUANTUM MECHANICAL PROBLEM

The exact quantum mechanical description of an explosive requires wave functions which contain all of the information about the states of the explosive. In a practical sense, however, it is impossible and, frequently, unnecessary to calculate such detailed information about the system. Moreover, even if exact wave functions or eigenfunctions of the Schrödinger wave equation could be obtained, they would be so complicated that many of the intuitive aspects of the fundamental interactions would be masked by the quantum mechanical nature of the dynamics. In this report, models and rigorous computational schemes are introduced which quantitatively approximate the states of highly compressed explosives, and yet maintain a reasonably simple picture of interacting explosive molecules.

Quantum mechanical treatments of the fundamental interactions between N electrons, N nucleons, N atoms, or N molecules have all begun with the averaged interactions of the N particles, where the motion of each particle is such that it moves in an averaged field generated by the remaining N-1 particles. A mathematical basis for this approach is contained in the Hartree-Fock theory,[17] which forms the theoretical framework for the shell structure of nuclei, atoms, and molecules. The shell model has had immense success as a quantitative and qualitative tool in the analysis of atoms and molecules. This theory is as far as one can go in utilizing the so-called orbital picture in atoms and molecules.

---

[16]Laidler, K. J., Chemical Kinetics (New York: McGraw-Hill Book Co., Inc., 1965), pp. 72-112.

[17]Slater, J. C., Quantum Theory of Atomic Structure, Volume II, (New York: McGraw-Hill Book Co., Inc., 1960), pp. 1-30.

*Frequently, plots of the free energy vs. reaction coordinate are used to analyze reaction paths. These plots represent the totality of energy changes occurring during reaction and already contain the potential energy changes ascribed to the reaction path imbedded in the hypersurface. The assumption of equilibrium between reactants and the activated species in the absolute reaction rate theory dispenses with the need to know the pathway taken to reach the activated state. Therefore, when this theory provides a good description of reactions, one need not be concerned with the complete potential energy hypersurface. In the Sections entitled, "The Quantum Mechanical Problem" and "Calculations of Ground and Excited States for the $(NO^+)_n$ Molecular System," the surfaces are treated in their entirety.

Methods which refine the Hartree-Fock theory have been introduced which not only improve the quantitative accuracy, but which also maintain intuitive pictures of molecular and nuclear structures. In the case of molecular electronic structure, the generalized valence bond[18] methods, for example, are finding increased usage in polyatomic molecules. These methods represent one aspect of the more general configuration interaction techniques which treat the correlation of motions of electrons and of nucleons. The generalized valence bond methods maintain the chemist's idea of the nature of a covalent bond containing two electrons. The considerable quantitative improvement which these methods achieve is ascribed to the treatment of the detailed interactions of any two electrons moving in the averaged field of the remaining N-2 electrons. Interestingly enough, even at the highest known densities of matter, nuclear theoretical techniques have demonstrated that major energy improvements are also achieved with a pairwise potential of two nucleons moving in the averaged N-2 nucleon field.[19] Higher-order corrections which provide for the correlation of the motions of electrons and of nucleons are required to obtain complete agreement with experiment; but, these corrections obscure the traditional shell structure and electron-pair pictures of matter.

The characterization of the dynamics of interacting molecules is often not as clearcut as the dynamics of electrons and nucleons, since strongly interacting molecules change the electronic structure of the individual molecules. A determination of equations of state requires interaction potentials. Jacobs[20] has determined that the equation of state of a strongly shocked solid explosive is closer to that of a liquid than a solid. Whereas liquids near the triple point are frequently analyzed satisfactorily in terms of pair potentials $\phi(i,j)$ between atoms and molecules, triplet potentials $\phi(i,j,k)$ and, perhaps, higher-order potentials are expected to be important at the high densities of shocked explosives where the total potential energy U_I for a given configuration of atoms or molecules would have the form

$$U_I = \sum_{i<j} \phi(i,j) + \sum_{i<j<k} \phi(i,j,k) + \text{higher-order terms} \quad . \qquad (8)$$

---

[18]Dunning, Jr., T. H., Cartwright, D. C., Hunt, W. J., Hay, P. J., and Bobrowicz, F. W., "Generalized Valence Bond Calculations on the Ground State ($X^1\Sigma^+_g$) of Nitrogen," Journal of Chemical Physics, Vol. 64, No. 11, 1976, p. 4755, and other references cited therein.

[19]Bethe, H. A., "Nuclear Many-Body Problem," Physical Review, Vol. 103, No. 5, 1956, p. 1353.

[20]Jacobs, S. J., "On the Equation of State for Detonation Products at High Density," in Twelfth Symposium (International) on Combustion, 1969, pp. 501-511.

The summations in Equation (8) refer to the atoms or molecules. The pair potential $\phi'(i,j)$, for example, would contain variables for the intermolecular distances and relative orientations of two molecules interacting in isolation from the other molecules. The actual pair potential $\phi(i,j)$ in the averaged field of the remaining molecules would be a simple function of $\phi'(i,j)$. Thus, a description of interacting molecules can be built up in a manner analogous to that done for electrons and nucleons. It will be shown in the Section entitled, "Calculations of Ground and Excited States for the $(NO^+)_n$ Molecular System," that the largest shifts in electronic excitation energies occur for three interacting NO^+ molecules so that $\phi(i,j)$ and $\phi(i,j,k)$ are adequate for a description of molecular electronic structure. The results of detailed calculations on the system of two interacting NO^+ molecules are presented in the Section entitled, "Calculations of Ground and Excited States for the $(NO^+)_n$ Molecular System," from which some idea of the nature of $\phi(i,j)$ is obtained. Triplet potentials $\phi(i,j,k)$ will be considered in a future report.

It is frequently desirable to treat the interacting molecules as an assemblage of electrons and nuclei which yield a potential energy U_{en}. Once the energy U_{en} is obtained, it may be used to evaluate the pressure P from the virial theorem equation of state,[21]

$$PV = \frac{2}{3}\bar{K} - \frac{1}{3}\sum_{i=1}^{M}\overline{\vec{r}_i \cdot \frac{\partial U_{en}}{\partial \vec{r}_i}} \quad , \tag{9}$$

where $\bar{K}$ is the average total kinetic energy, M is the number of electrons and nuclei in the molecular composite with potential energy U_{en}, and $\vec{r}_i$ is a vector locating the position of particle i. Since we are concerned here with electrostatic forces among the electrons and nuclei, the averaged quantity in the second term of Equation (9) becomes

$$-\sum_{i=1}^{M}\overline{\vec{r}_i \cdot \frac{\partial U_{en}}{\partial \vec{r}_i}} = \overline{U_{en}} \quad . \tag{10}$$

Note that the second term of Equation (9) will be nonzero at 0^oK so that P may be written*

$$P = P_T(V,T) + P_0(V) \quad . \tag{11}$$

---

[21]Hirschfelder, J. O., Curtiss, C. F., and Bird, R. B., Molecular Theory of Gases and Liquids, (New York: John Wiley & Sons, Inc., 1954), pp. 134-135.

*Jacobs[20] and Pastine[5] have used Equation (11), which also follows from the Grüneisen equation of state.

Equations (9) and (10) may be simplified by invoking the Born-Oppenheimer (BO) approximation which is permitted by the separation of electronic and nuclear motions. In this approximation, Slater[22] showed that

$$\bar{K}_e = - E_e - \sum_{\text{nuclei}} \vec{r}_i \cdot \frac{\partial E_e}{\partial \vec{r}_i} \tag{12}$$

and

$$\bar{K}_e + \bar{U}_{en} = E_e \quad , \tag{13}$$

where $\bar{K}_e$ is the quantum mechanical expectation value of the electronic kinetic energy, and E_e includes the total electronic energy and the nuclear repulsion energy. Since $\bar{K} = \bar{K}_e + \bar{K}_n$, substitution of Equations (12) and (13) into Equation (9) yields

$$PV = \frac{2}{3} \bar{K}_n - \frac{1}{3} \sum_{\text{nuclei}} \vec{r}_i \cdot \frac{\partial E_e}{\partial \vec{r}_i} \quad . \tag{14}$$

It is seen here that E_e is now the potential for nuclear motion to be used in the determination of P. E_e is determined from the electronic structure of the entire assemblage of interacting molecules, as is done in the so-called "supermolecule" approach to intermolecular interactions.[23] We now turn to an analysis of the nature of E_e and the BO approximation.

Bardo and Wolfsberg[10] have shown that the nonrelativistic Schrödinger wave equation in a coordinate system rotating with a molecular system can be written in the form

$$(T+V-E)\psi_s^J + T_+\psi_{s+1}^J + T_-\psi_{s-1}^J$$

$$+ T_{++}\psi_{s+2}^J + T_{--}\psi_{s-2}^J = 0 \quad ,$$

$$s = -J, -J+1, \cdots J \quad . \tag{15}$$

---

[22]Slater, J. C., Quantum Theory of Molecules and Solids, Volume I, (New York: McGraw-Hill Book Co., Inc, 1963), pp. 29-40.

[23]Amos, A. T., and Crispin, R. J., "Calculations of Intermolecular Interaction Energies," in Eyring, H., and Henderson, D., eds., Theoretical Chemistry, Advances and Perspectives, Vol. 2, (New York: Academic Press, 1976), pp. 33-35.

In this set of (2J + 1) coupled equations, J and s are the quantum numbers of the total angular momentum and the projection of the total angular momentum onto the z-axis of a rotating coordinate system, respectively. T, T_+, T_-, T_{++}, and T_{--} are kinetic energy operators, the forms of which depend on the choice of coordinate system rotating with the molecular system. T_+, T_-, T_{++}, T_{--} arise from the Coriolis-like interactions between the rotational, electronic, and vibrational motions. V is the usual expression for the potential energy which includes the electrostatic potential energy terms among electrons and the N nuclei. E is the total energy (excluding the energy of the center-of-mass motion) of the rotational and internal motions of the system.

Equation (15) strictly applies to the entire assemblage of molecules in an explosive for which J is a good quantum number and, in principle, provides an exact nonrelativistic quantum mechanical solution for the explosive in any given state. Each wave function ψ_s^J may be expanded in terms of a complete set of orthonormal electronic wavefunctions,

$$\psi_s^J = \sum_K F_{Ks}^J \, \Phi_K \quad , \tag{16}$$

where F_{Ks}^J is a function of the 3N-6 coordinates of the nuclei, and Φ_K is a function of these nuclear coordinates and the coordinates of the electrons. The functions Φ_K are orthonormal in the sense that

$$\int \Phi_K^* \, \Phi_L \, dv_{\text{electrons}} = \delta_{KL} \quad . \tag{17}$$

Substituting Equation (16) into Equation (15), multiplying on the left by $\Phi_{K'}^*$, and integrating over the electronic coordinates, we have

$$\langle \Phi_{K'} | T+V | \Phi_{K'} \rangle F_{K's}^J - EF_{K's}^J + \langle \Phi_{K'} | T_+ | \Phi_{K'} \rangle F_{K',s+1}^J \tag{18}$$

$$+ \langle \Phi_{K'} | T_- | \Phi_{K'} \rangle F_{K',s-1}^J + T_{++} F_{K',s+2}^J + T_{--} F_{K',s-2}^J =$$

$$- \sum_{K(\neq K')} \left\{ \langle \Phi_{K'} | T+V | \Phi_K \rangle F_{Ks}^J + \langle \Phi_{K'} | T_+ | \Phi_K \rangle F_{K,s+1}^J + \langle \Phi_{K'} | T_- | \Phi_K \rangle F_{K,s-1}^J \right\} .$$

The bracket notation $\langle | \, | \rangle$ of Dirac used here denotes integration over the electronic space and spin coordinates only.

The solution of Equation (18) is greatly simplified when the functions Φ_K are chosen in such a way that the number of terms in the summations in Equations (16) and (18) is as small as possible. For many physical problems, extremely rapid convergence has been obtained when the functions Φ_K were chosen as electronic states within the framework of the BO approximation, Φ_K^{BO}. In this approximation, each state ψ_s^J of the molecular system is very well approximated by

$$\psi_s^J \simeq F_{Ls}^J \Phi_L^{BO} \quad , \tag{19}$$

where L denotes additional, good quantum numbers which arise from the approximation and which distinguish electronic states, but which are nonexistent in the exact solution represented by ψ_s^J.

The equations of the BO approximation are obtained from the exact equations, Equation (18). It was shown in Reference 10 that the operators T and $T_\pm$ contain derivatives with respect to only nuclear coordinates. In hartree units (1 hartree = 27.2 ev), the operator T may be written as

$$T = T' - \tfrac{1}{2} \sum_n \nabla_n^2 \quad , \tag{20}$$

where the sum over n is for the electrons, and ∇_n^2 is the electronic Laplacian. The operators T', $T_\pm$ and $T_{\pm\pm}$ contain terms involving first and second partial derivatives, and involving the reciprocal of the i-th nuclear mass, $m_{nucl,i}^{-1}$. One such term, for example, is $(m_{nucl,i}^{-1})(\partial^2/\partial x \partial R_k)$ where R_k is an internuclear distance and x is an electronic Cartesian coordinate. The BO approximation, then, utilizes the large ratio of the nuclear mass to the electronic mass, and the slow variation of the electronic wave function Φ_K^{BO} with a nuclear displacement of less than a bohr radius a_0 (a_0 = 0.529 Å),

$$\left| \frac{\partial \Phi_K^{BO}}{\partial R_k} \right| \lesssim a_0^{-1} |\Phi_K^{BO}| \quad , \tag{21}$$

where R_k is an internuclear distance and $\partial/\partial R_k$ is a derivative contained in T', and in $T_\pm^N = T_\pm - T_\pm^e$. $T_\pm^N$ and $T_\pm^e$ refer to only the nuclear coordinates and the electronic coordinates, respectively. T' and $T_\pm^e$ also contain terms with electronic orbital angular momentum operators and $m_{nucl,i}^{-1}$. Consequently, the operations $T'\Phi_K^{BO}$ and $T_\pm \Phi_K^{BO}$ are small so that Equation (18) becomes

$$(T'+E_K^{BO}-E)F_{Ks}^J + T_+^N F_{K,s+1}^J + T_-^N F_{K,s-1}^J$$

$$+ T_{++} F_{K,s+2}^J + T_{--} F_{K,s-2}^J = 0 \quad , \tag{22}$$

where we have let

$$\langle \Phi_K^{BO} | -\tfrac{1}{2} \sum_n \nabla_n^2 + V | \Phi_K^{BO} \rangle = E_K^{BO} \tag{23}$$

or

$$H_e \Phi_K^{BO} \equiv (-\tfrac{1}{2} \sum_n \nabla_n^2 + V) \Phi_K^{BO} = E_K^{BO} \Phi_K^{BO} \quad . \tag{24}$$

Equations (22) and (24) are the eigenvalue equations of the BO approximation.

These two equations represent a great simplification of the solution to the molecular problem, since the electronic motion described by Equation (24) is treated independently of the nuclear motion described by Equation (22). The eigenvalues E_K^{BO} are functions of the 3N-6 nuclear coordinates where N is the number of nuclei. Equation (24) is solved for each configuration of fixed nuclei. Thus, for each such rigid configuration, the electrons move throughout the framework of nuclei and establish a force field described by Φ_K^{BO} and E_K^{BO} which acts on the nuclei.[24] Since the positions of the nuclei are fixed in the solution of Equation (24), E_K^{BO} is a potential energy function for nuclear motion. This, of course, is already implied in the structure of the operator $T' + E_K^{BO}$ in Equation (22), the solution of which gives the vibrational motions of the nuclei described by the wave functions F_{Ks}^J, $F_{K,s\pm1}^J$, and $F_{K,s\pm2}^J$. For each total energy eigenvalue E, $E - E_K^{BO}$ is the vibrational energy.

Each function of the nuclear coordinates E_K^{BO} is what is often referred to as an electronic state. The electronic state can pertain to a composite of molecules in the condensed phase, or to a single molecule in the gas phase. Graphs of these functions in nuclear coordinate space reveal that there is generally one function which gives energy values all lying below the energy values

---

[24]Feynman, R. P., "Forces in Molecules," Physical Review, Vol 56, 1939, p.340.

corresponding to the other functions. This lowest function is called the ground electronic state, E_0^{BO}. All higher-lying functions E_1^{BO}, E_2^{BO}, ... are called excited electronic states. The K-th graph of the function E_K^{BO} is a hypersurface which is a potential energy surface. This is the surface mentioned in the Section entitled "The Activation Energy as a Potential Energy Concept." In the case of two interacting atoms, as in a diatomic molecule or solid, E_K^{BO} is a curve (1-dimensional surface) which is frequently approximated by a Morse potential, a Lennard-Jones (6-12) potential, or a Buckingham potential.[21]

Equation (24) may be solved for a system of reacting molecules. Here the function E_K^{BO} gives a surface which describes the reaction as it proceeds from reactants through the activated state to the products. The reacting system is envisioned as a mathematical point moving along some path which originates at a low point, the position of the reactants, on the surface and continues through valleys between mountains and over a pass into another low point, the position of the products, on the surface. The surface can reveal the most probable course of the reaction without having to introduce the motions of the nuclei through the solution of Equation (22). Unfortunately, the generation of a complete hypersurface for an electronic state, as it applies to the total assemblage of molecules or to even a few reacting molecules within the assemblage, constitutes an intractable computational problem. Considerable expense has been incurred in the case of quantum mechanical calculations on three interacting hydrogen molecules.[25] Frequently, the hypersurfaces for interacting and reacting molecules are approximated by elaborate potentials which contain Morse potential terms and exponential repulsion terms with coefficients which modify the attractive parts of Morse potentials so that exothermicity in reactions is achieved. These potentials have been used in conjunction with Monte-Carlo calculations on reaction trajectories.[26]

It is often unnecessary to consider hypersurfaces in their entirety. For example, the analysis of the breaking of a single bond in a molecule may be carried out by examining a cut-out of the surface which corresponds to the variation of a single bond distance. In the case of the sensitivity of an explosive, the bond-breaking process may be in some cases the most important step in the reaction mechanism for initiation of detonation. It is this process which is to be examined in detail in this report.

---

[25]Ross, M., and Shishkevish, C., "Molecular and Metallic Hydrogen," R-2056-ARPA, 1977.

[26]Blais, N. C., and Bunker, D. L., "Monte Carlo Calculations.II. The Reactions of Alkali Atoms with Methyl Iodide," Journal of Chemical Physics, Vol. 37, No. 11, 1962, p. 2713. See also Karo, A. M., and Hardy, J. R., "Molecular Dynamics of Shock-Initiated Detonations," International Journal of Quantum Chemistry, Vol. 12, Suppl. 1, 1977, p. 333.

The BO approximation is really a semiclassical treatment made possible by the large nuclear-to-electron mass ratio. The solution of Equation (24) constitutes a violation of the quantum mechanical nature of motions of nuclei, since the nuclei are held in fixed positions, giving each nucleus a simultaneously known position and velocity (velocity = 0) which violates the uncertainty principle. It is this aspect which permits the use of Monte-Carlo calculations in the analysis of reaction mechanisms. As long as single surfaces E_K^{BO} are sufficient for describing reactions, the BO approximation is valid to a high degree of approximation. The semiclassical treatment is less accurate when the molecules contain nuclei of small mass. Such is the case for isotopic exchange reactions involving the hydrides and deuterides, where quantum mechanical effects due to the interactions of nuclear and electronic motions become important. Here, the interactions are contained in a first-order correction term

$$C_K = \langle \Phi_K^{BO} | T' | \Phi_K^{BO} \rangle \quad , \tag{25}$$

which was dropped in Equation (22), but which adds on to E_K^{BO} when the BO approximation no longer holds. Since the BO approximation is frequently referred to as an adiabatic theory, C_K is called the adiabatic correction, since a new potential energy surface $E_K^{BO} + C_K$ is considered. [27]

So far we have considered only those physical situations where the surfaces E_K^{BO} are sufficiently far apart so that only one surface is needed in the analysis of a given reaction. It is frequently found, however, that the shapes of the surfaces vary enough with nuclear configuration so that two or more surfaces come close to intersecting or, in fact, do intersect. The situation where two curves closely approach each other without actually crossing is often referred to as an "avoided crossing." If two surfaces intersect at a point corresponding to a particular configuration of the nuclei, we have the condition

$$E_K^{BO} = E_{K'}^{BO} \quad . \tag{26}$$

---

[27] Bardo, R. D., and Wolfsberg, M., "A Theoretical Calculation of the Equilibrium Constant for the Isotopic Exchange Reaction between H_2O and HD," Journal of Physical Chemistry, Vol. 80, No. 10, 1976, p. 1068. It was shown in this paper that the adiabatic correction leads to equilibrium constants which differ from the experimental ones by less than the experimental error.

Teller[28] has shown that the shapes of two surfaces in the neighborhood of an intersection define a double cone when each surface E_K^{BO} is a function of two parameters. More complicated types of intersections are discussed by Carrington.[29] These intersections can have a profound effect on reactions since the BO approximation breaks down and Equations (21), (22), and (24) no longer apply. Here we find that the semiclassical approach fails, and that the quantum mechanical effects manifest themselves completely in Equation (18).

The theory of radiationless transitions[30] is based on the intersections of surfaces. Intersections among the excited state surfaces are much more prevalent than among these surfaces and the ground state surface. Hence, radiationless processes (e.g., predissociation) and photochemical reactions frequently involve excited electronic states. For these reactions, electronic excitation is first required to reach an excited state from which the radiationless transition occurs. It will be demonstrated later that surfaces belonging to excited electronic states intersect ground state surfaces during compression and, therefore, may affect the nature of the bond-breaking reaction during initiation.

The separation between two surfaces E_1^{BO} and E_2^{BO} is given by

$$\Delta E = \sqrt{(H_{11}-H_{22})^2 + 4H_{12}^2} \quad , \tag{27}$$

where H_{ij} is the matrix element

$$H_{ij} = \langle \Psi_i | H_e | \Psi_j \rangle \quad . \tag{28}$$

H_e is the electronic hamiltonian of Equation (24). The eigenfunctions Φ_1^{BO} and Φ_2^{BO} belong to the symmetry group of H_e. The wave functions Ψ_i and Ψ_j are basis functions. Longuet-Higgins[31] has proven that the necessary and sufficient conditions for an intersection, $\Delta E = 0$, of two surfaces to occur are, from Equation (27),

---

[28]Teller, E., "The Crossing of Potential Surfaces," Journal of Physical Chemistry, Vol. 41, No. 1, 1937, p. 109.

[29]Carrington, T., "The Geometry of Intersecting Potential Surfaces," Accounts of Chemical Research, Vol. 7, 1974, p. 20.

[30]Jortner, J., Rice, S. A., and Hochstrasser, R. M., "Radiationless Transitions in Photochemistry," in Noyes, W. A. et al., eds., Advances in Photochemistry, Vol. 7, (New York: Wiley, 1969), pp. 149-309.

[31]Longuet-Higgins, H. C., "The Intersection of Potential Energy Surfaces in Polyatomic Molecules," Proceedings of the Royal Society, London, Vol. A344, 1975, p. 147.

$$H_{11} = H_{22} \quad , \quad H_{12} = 0 \quad . \tag{29}$$

In general,

$$H_{11}-H_{22} = G \quad , \quad H_{12} = G' \quad , \tag{30}$$

where both G and G' are functions of all of the nuclear coordinates. If these coordinates are internuclear distances and one distance is varied while all others are fixed, a curve is generated which is imbedded in the surface under consideration. Von Neumann and Wigner[32] introduced the noncrossing rule for two such curves when they showed that $H_{12} \neq 0$ when the basis functions Ψ_i and Ψ_j have the same symmetry (spin, parity, angular momentum) so that ΔE never vanishes. In the case of a diatomic molecule, there is only one internuclear distance parameter for which it is impossible to satisfy both conditions in Equation (29) by solving the two equations, Equation (30), simultaneously.[33] In the case of a polyatomic molecule with two or more independent internuclear distance parameters, at least two of these parameters may be found which satisfy the two conditions of Equation (29) simultaneously. If H_{12} is complex when, for example, magnetic forces are important, additional parameters are introduced. Hence, at least as far as the geometrical parameters are concerned, intersections between two surfaces corresponding to electronic states of the same symmetry may occur for polyatomic molecules, as opposed to the situation for diatomics. The major point here is that there are no symmetry restrictions in polyatomic molecules which would prevent the intersections of surfaces, so that one may expect intersections to be prevalent in large molecules. When diatomic molecules interact with each other at high compressions, one must really consider the system to be a "supermolecule" which is, effectively, a "polyatomic molecule." The noncrossing rule may break down for diatomics at high compressions.

---

[32]von Neumann, J. and Wigner, E., "Uber das Verhalten von Eigenwerten bei adiabatischen Prozessen," Zeitschrift für Physik, Vol. 30, 1929, p. 467.

[33]Hatton, G. J., "The Noncrossing Rule and Spurious Avoided Crossings," Physical Review A, Vol. 14, No. 3, 1976, p. 901. Hatton has suggested that there may be dynamical symmetries besides the spatial and spin symmetries which establish additional relationships among matrix elements, even though the states involved have the same spatial and spin symmetries. Here, the traditional noncrossing rule of von Neumann and Wigner would no longer be applicable. The condition $H_{12} = 0$ exists for all symmetries as a consequence of the following important theorem: If there exists a complete set of commuting operators which includes H_e, and Ψ_i and Ψ_j are eigenfunctions of at least one operator (not H_e), then $H_{12} = 0$ unless the two eigenvalues a_i and a_j satisfy $a_i = a_j$.

Equation (21) is no longer satisfied when the eigenfunctions Φ_K of H_e in Equation (24) vary rapidly near an "avoided crossing." Here, the designation BO has been dropped since it no longer applies to Φ_K and E_K when the matrix elements $\langle \Phi_{K'} | T'+T_++T_- | \Phi_K \rangle$ in Equation (18) are no longer negligible. However, a new set of basis functions $\{\bar{\Phi}_K\}$ may be found which are different from Φ_K and which satisfy

$$\left| \frac{\partial \bar{\Phi}_K}{\partial R_k} \right| \leq a_0^{-1} |\bar{\Phi}_K| \quad . \tag{31}$$

The wave functions $\bar{\Phi}_K$ are no longer eigenfunctions of H_e, but still allow a separation of motions of nuclei and electrons. In this case, Equation (18) becomes

$$\begin{aligned} (T'+\mathcal{E}_{K'K'}-E)\bar{F}^J_{K's} + T^N_+\bar{F}^J_{K',s+1} + T_-\bar{F}^J_{K',s-1} \\ + T_{++}\bar{F}^J_{K',s+2} + T_{--}\bar{F}^J_{K',s-2} \\ = -\sum_{K(\neq K')} \mathcal{E}_{K'K}\bar{F}^J_{Ks} \end{aligned} \tag{32}$$

where

$$\langle \bar{\Phi}_{K'} | H_e | \bar{\Phi}_K \rangle = \mathcal{E}_{K'K} \quad . \tag{33}$$

It is noted here that

$$\Phi_K = \sum_L U_{KL}\bar{\Phi}_L \quad , \tag{34}$$

where the coefficients U_{KL} comprise a unitary transformation, and are functions of the nuclear coordinates. When the nuclear configurations are far removed from the one at the "avoided crossing," $U_{KL} = \delta_{KL}$.

Diagrams of an "avoided crossing" for two curves are presented in Figure 1a. Figure 1a shows the situation when the two curves E_1 and E_2 closely approach each other and bend sharply away. The derivative in Equation (21) is large in the region of closest approach. In Figure 1b, the new choice of $\bar{\Phi}_1$ and $\bar{\Phi}_2$ smooths out the curves and leads to an intersection, $\mathcal{E}_{11} = \mathcal{E}_{22}$. Equation (31) is obeyed in Figure 1b.

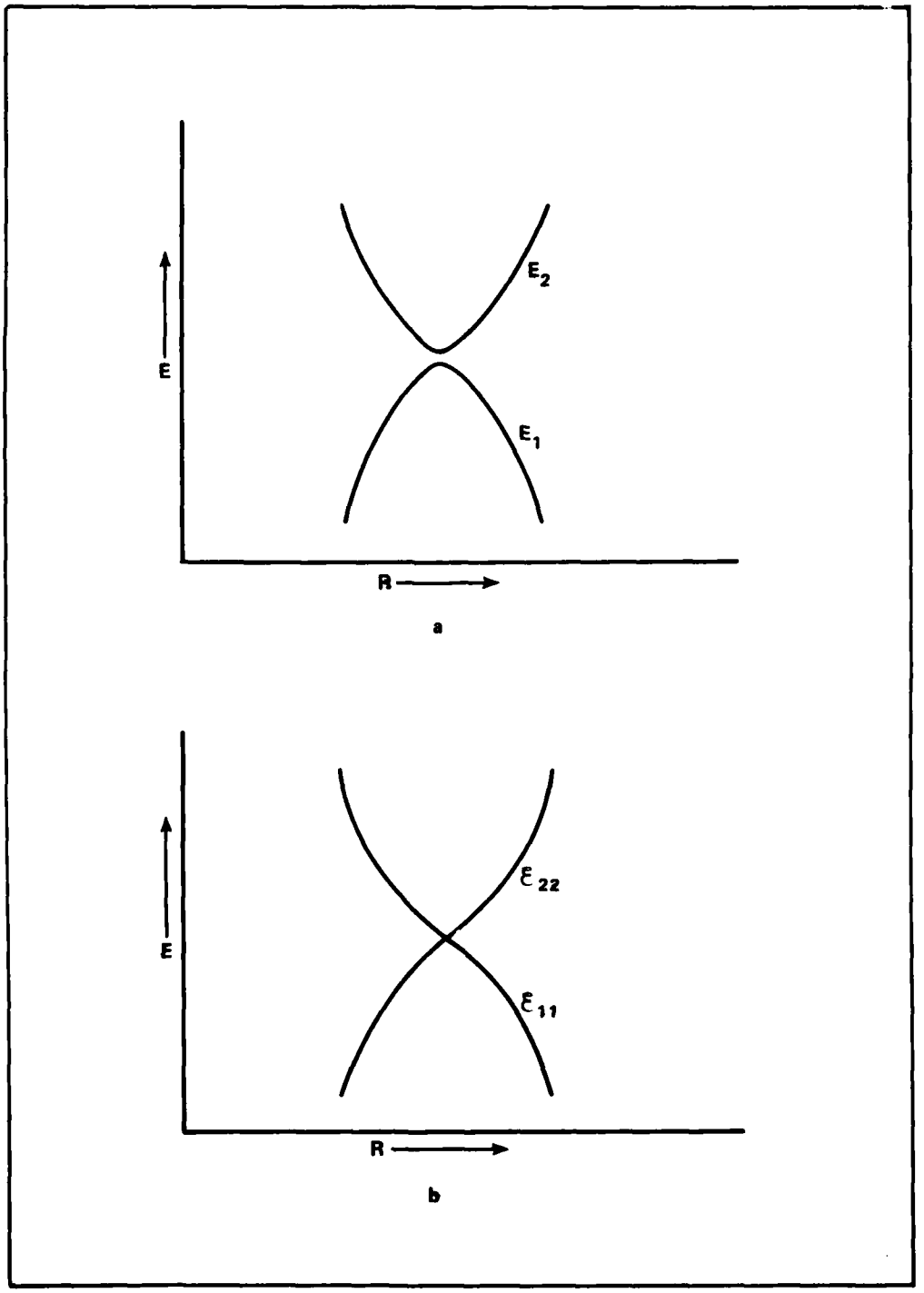

FIGURE 1 AVOIDED CROSSING AND INTERSECTION FOR TWO POTENTIAL ENERGY CURVES

It is apparent from Equations (32) and (33) that the potential energy "seen" by the nuclei has meaning only when the kinetic energy of the nuclei is considered and, therefore, only with respect to the total energy E attained. If E has values close to $\mathcal{E}_{KK}(=\mathcal{E}_{LL})$, the molecular system has a good chance of "escaping" through an intersection and of achieving nuclear configurations beyond the intersection by moving on E_K. Here, the system may have sufficient time to adjust even though $|\partial\Phi_K/\partial R_k|$ may be large. On the other hand, if E has values close to $E_K(=E_L)$, which is an intersection for the eigenvalues of Equation (24), the system has a good chance of "escaping" on $\mathcal{E}_{KK}$ to nuclear configurations beyond the intersection even though $|\partial\bar{\Phi}_K/\partial R_k|$ may be large. When E is much larger or much smaller than $\mathcal{E}_{KK}=\mathcal{E}_{LL}$, the surface "selected" for the most probable motion is either E_K or E_L.

The concept of the probability of "surface hopping," which was dexcribed in the previous paragraph, was introduced by Zener,[34] and Landau,[35] and Stückelberg,[36] and is discussed by Eyring, et al.[37] within the context of the general theory of reaction rates. These authors consider two surfaces given by E_1 and E_2 of the molecular system "hopping" from E_1 to E_2, $E_1<E_2$. Using the wave functions and energies defined previously in this report, we have at $\mathcal{E}_{11} = \mathcal{E}_{22}$,

$$\Phi_{1,2} = \frac{1}{\sqrt{2}}\left(\bar{\Phi}_1 \pm \bar{\Phi}_2\right) \tag{35}$$

and

$$H_e\bar{\Phi}_1 = \mathcal{E}_{11}\bar{\Phi}_1 - \mathcal{E}_{12}\bar{\Phi}_2 \quad , \tag{36}$$

$$H_e\bar{\Phi}_2 = \mathcal{E}_{22}\bar{\Phi}_2 - \mathcal{E}_{12}\bar{\Phi}_1 \quad , \tag{37}$$

where $\mathcal{E}_{KL}$ is given by Equation (33). The expression for the probability of "surface hopping," the transition probability, is

---

[34]Zener, C., "Non-Adiabatic Crossing of Energy Levels," Proceedings of the Royal Society of London, Ser. A, Vol. 137, 1932, p. 696.

[35]Landau, L. D., and Lifshitz, E. M., Quantum Mechanics, 2nd Edition (Reading, Mass.: Addison-Wesley Publishing Co., Inc., 1965), pp. 322-330.

[36]Stückelberg, E. C. G., "Theorie der Unelastischen Stösse Zwischen Atomen," Helvetica Physica Acta, Vol. 5, 1932, p. 369.

[37]Eyring, H., Walter, J., and Kimball, G. E., Quantum Chemistry (New York: John Wiley & Sons, Inc., 1944), pp. 299-331.

$$P = \exp\left[-\frac{4\pi^2\mathcal{E}_{12}^2}{hv|s_1-s_2|}\right] \tag{38}$$

where h is Planck's constant, v is the nuclear velocity along a curve, and $s_1 = \partial\mathcal{E}_{11}/\partial R_k$, $s_2 = \partial\mathcal{E}_{22}/\partial R_k$ are the slopes evaluated at the nuclear configuration where $\mathcal{E}_{11} = \mathcal{E}_{22}$. The probability that the system stays on E_1 is

$$P' = 1-P \quad . \tag{39}$$

Equations (38) and (39) tell us that for a high nuclear velocity and a small separation of curves, $|2\mathcal{E}_{12}|$, at the "avoided crossing," the probability is large that the system "hops," and that P' is small. Equations (38) and (39) continue to apply when the surfaces E_1 and E_2 themselves intersect when, for example, Φ_1 and Φ_2 are of different symmetry.

The preceding discussion of "avoided crossings" was concerned with surfaces E_K and $E_{K'}$ which are the eigenvalues in Equation (24). The corresponding eigenfunctions Φ_K and $\Phi_{K'}$ have the same symmetry so that the noncrossing rule is obeyed. Equations (31) - (39) arose as a consequence of the system being able to "hop" from E_K to $E_{K'}$. In the case of an intersection $E_K = E_{K'}$, Φ_K and $\Phi_{K'}$ will usually satisfy Equation (21), but not Equation (22). At the intersection $E_1 = E_2$, degenerate perturbation theory is used which involves diagonalizing a two-dimensional matrix with matrix elements $\langle\Phi_i|T'+T_+ +T_-|\Phi_j\rangle$. This procedure yields two new wave functions

$$\Psi_1 = U'_{11}\Phi_1 + U'_{12}\Phi_2 \quad , \tag{40}$$

$$\Psi_2 = U'_{21}\Phi_1 + U'_{22}\Phi_2 \quad . \tag{41}$$

These wave functions are associated with two new surfaces which do not intersect. It should be pointed out that the unitary transformation of Equations (40) and (41) is, in general, different from that defined in Equation (34). The transformation in Equation (34) defines the wave functions $\bar{\Phi}_1$ and $\bar{\Phi}_2$ which minimize $\langle\bar{\Phi}_1|T'+T_+ +T_-|\bar{\Phi}_2\rangle$ so that Equation (32) is satisfied. Diagonalization of the matrix itself does not guarantee the smallness of matrix elements in the different basis set. A complete analysis of a given physical problem requires the use of the exact wave equations, Equation (18), in a perturbation treatment. Once a given set of surfaces is specified, Equations (38) and (39) are applicable. In general, the matrix element $\mathcal{E}_{12}$ in Equation (38) is given by

$$\hat{\mathcal{E}}_{12} = \langle \Psi_1 | T' + T_+ + T_- | \Psi_2 \rangle \qquad (42)$$

and not Equation (33). In a future report, we consider the mathematical development and computation of $\hat{\mathcal{E}}_{12}$.

The importance of the preceding discussion for the shock initiation process is that compression shifts and warps surfaces and, consequently, may create intersections among the excited state surfaces E_1, E_2, ... and the ground state surface E_0, or bring the surfaces into close proximity. New channels for reaction may be created in the process. As a consequence, alterations of the surfaces will be manifested in changes in reaction kinetics and in frequency and bandwidth shifts for infrared, visible, and ultraviolet spectra. If by excited and ground state surfaces we mean those of the isolated molecule, then the compression shifts and warps these surfaces in a perturbative sense as the molecules approach each other. If we mean that the surfaces belong to a composite system of molecules, the surfaces for the composite will also be shifted and warped to an extent depending on the state of compression. At high compressions, one can really consider only the surfaces for the composite system. In this case, a perturbation analysis yields either slow convergence or divergence. However, an "effective or average set of surfaces per molecule" may be defined by dividing the energies E_K by the number of molecules in the composite.

The shifting of existing intersections and the creation of new intersections will change activation energies from their values found under ambient conditions. These activation energies correspond to the ones discussed in the Section entitled "The Activation Energy as a Potential Energy Concept" and designated there as $E^{int.}_{act,i}$ in Equation (7). The solutions of Equation (24), which yield surfaces at various stages of compression of a molecular system, can be used to compute activation energies which are accurate to within 10% of the real values. For example, a possible activation energy is

$$E^{int}_{act,i} \simeq E_0(X) - E_0(0) \quad , \qquad (43)$$

where $E_0(X)$ and $E_0(0)$ are the eigenvalues of Equation (24) at the nuclear configurations corresponding to the activated system at the intersection and to the reactants at equilibrium, respectively. In order to obtain elementary activation energies to a higher degree of accuracy, and to complete the description of the reaction kinetics, higher-order contributions must be generated from Equation (18). These contributions would yield $\hat{\mathcal{E}}_{12}$ (Equation (42)) for use in Equations (38) and (39). Then, when the rate coefficient k_i is expressed as

$$k_i \propto \frac{\int_0^\infty P' \exp\left(-\frac{mv^2}{2kT}\right)dv \exp\left(-\frac{E_{act,i}^{int}}{kT}\right)}{\int_0^\infty \exp\left(-\frac{mv^2}{2kT}\right)dv} \quad , \qquad (44)$$

we have a description of the reaction in terms of the activation energy $E_{act,i}^{int}$, and of the probability P', Equation (39), averaged over the velocities v. $E_{act,i}^{int}$ in Equation (44) is the activation energy per molecule. In the case of an intersection $E_0 = E_1$, Equation (44) indicates that, for a given nuclear velocity v and a slope difference $|s_1-s_2|$, an increase in $\mathcal{E}_{12}$ and a corresponding decrease in $E_{act,i}^{int}$ greatly increases reaction rates. This is the behavior which may yield the fast reactions in detonations.

It is seen that the analysis consists of two parts. First, Equation (24) is solved which yields E_K at various compressions. The existence of an intersection $E_K = E_{K'}$ permits the determination of a good approximation to the activation energy given by Equation (43). Second, the utilization of perturbation theory in conjunction with Equation (42) refines the picture in terms of Equation (44). In the next section, the effects of compression on E_K are analyzed, and $E_{act,i}^{int}$ is evaluated for the system of interacting NO^+ molecules.

CALCULATIONS OF GROUND AND EXCITED STATES FOR THE $(NO^+)_n$ MOLECULAR SYSTEM

The solutions to Equation (24) are obtained by configuration interaction (CI) methods. Such solutions are of much higher accuracy than is often needed in calculations, and are obtained at great computer expense. Frequently, one looks for techniques which reveal as much information as is required for lower cost. Some of these techniques are briefly discussed in Appendix A. Instead of solving Equation (24), these methods yield solutions Ψ_K to the new eigenvalue equation

$$(H_e - V + V_{app})\Psi_K = \mathcal{E}_K \Psi_K \quad , \qquad (45)$$

where V_{app} is an approximate potential energy operator. V_{app} gives the interaction of single electrons with averaged fields in the case of the LCAO-MO-SCF method[38] or the interaction of electrons which modify the averaged fields in the case of the CNDO/S-CI method.[39] The meanings of the acronyms are given in Appendix A. Calculations are now discussed which utilize these methods to provide solutions to Equation (45) at relatively low cost.

The molecular system to be considered in this report is $(NO^+)_n$ where NO^+ is the closed-shell counterpart of the explosive open-shell NO molecule, and n is the number of molecules required to simulate compressed states. The system $(NO^+)_n$ is really a supermolecule on which LCAO-MO-SCF and CNDO/S-CI calculations are carried out.

The $(NO^+)_n$ molecular system represents a compromise between the NO explosive and the more common explosive molecular system. A description of the NO liquid explosive is complicated by dimerization.[40] However, most explosive molecules have closed shells and, therefore, do not dimerize under ambient conditions. The more complicated theoretical problem concerning $(NO)_n$ will be considered in a future report.

The CNDO/S-CI method was used on $(NO^+)_n$, n = 1,2,3,4,5, and 6, in order to ascertain the number of molecules required to yield the largest shifts in electronic excitation energies. Various configurations of NO^+ molecules were considered in each grouping. The results of the calculations are displayed in Figure 2 where the excitation energies $\Delta\mathcal{E}$ from the ground state to the lowest excited state are plotted against n. The graphs represent the variation of $\Delta\mathcal{E}$ in kcal per mole of supermolecules $(NO^+)_n$. In all calculations, the N-O bond distance in NO^+ was fixed at its equilibrium gas phase value of 1.062Å. The straight line pertains to all NO^+ molecules separated by distances greater than 3Å between nearest atoms, regardless of molecular orientation. The 3Å distance is a lower bound to that found in the condensed system at ambient pressures. This line proves that under normal conditions the condensed phase spectra are almost identical to gas phase spectra. The remaining curves indicate the variability of $\Delta\mathcal{E}$ for NO^+ molecules in linear

---

[38]Roothaan, C. C. J., "New Developments in Molecular Orbital Theory," Reviews of Modern Physics, Vol. 23, No. 2, 1951, p. 69.

[39]Del Bene, J., and Jaffé, H. H., "Use of the CNDO Method in Spectroscopy. I. Benzene, Pyridine, and the Diazines," Journal of Chemical Physics, Vol. 48, No. 4, 1968, p. 1807, and references cited therein.

[40]Ohlsen, J. R., and Laane, J., "Characterization of the Asymmetric Nitric Oxide Dimer O = N - O = N by Resonance Raman and Infrared Spectroscopy," Journal of the American Physical Society, Vol. 100, No. 22, 1978, p. 6948.

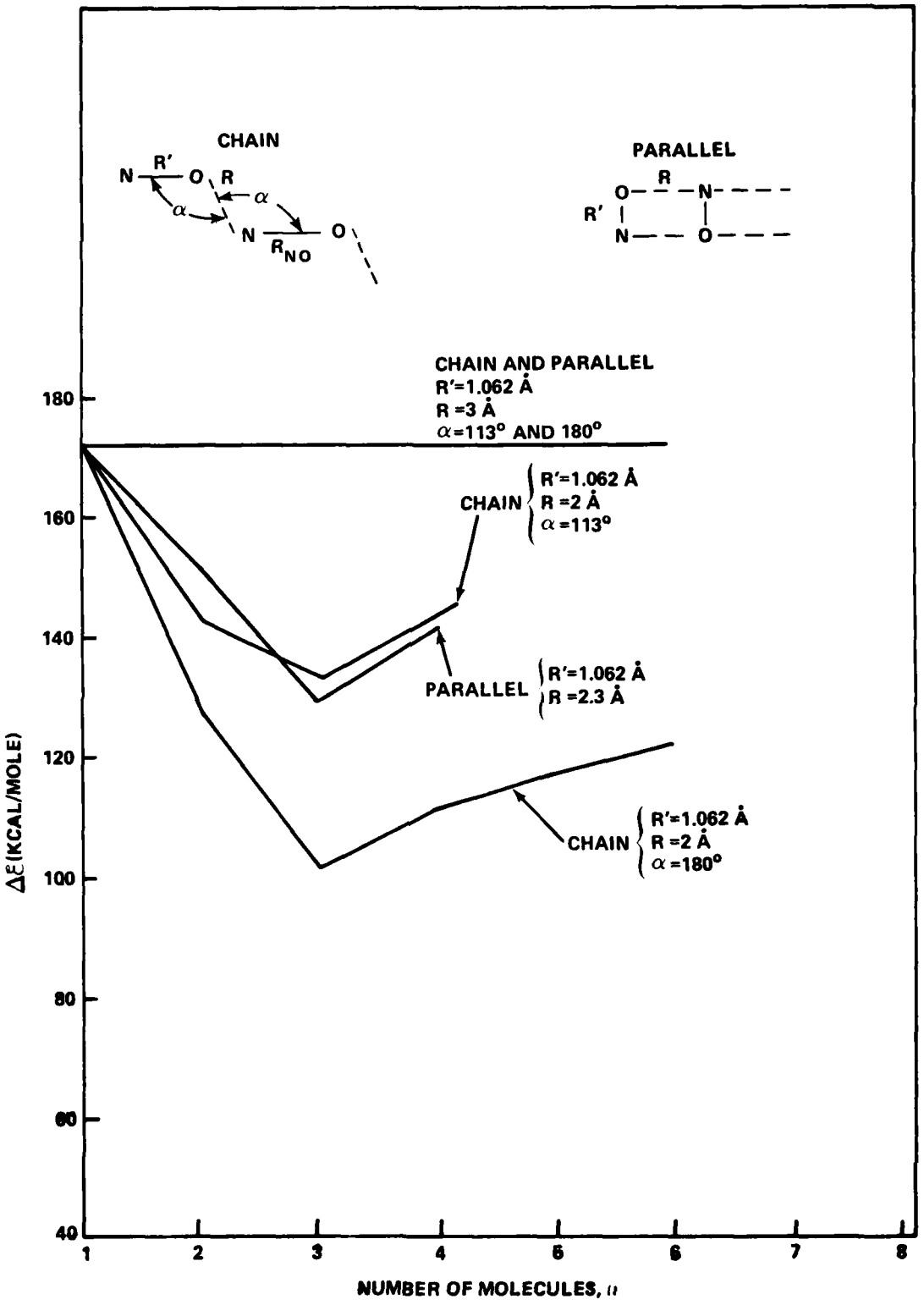

FIGURE 2 EXCITATION ENERGIES FOR $(NO^+)_n$

and zigzag chains where the nearest atoms of neighboring molecules are separated by R = 2Å. The nearest neighbor distance for the parallel system is R = 2.3Å. In the linear and zigzag chains, the R = 2Å separation corresponds to distances of nearly 3Å between the centers-of-mass of the individual molecules. It will be shown later that this separation corresponds to a pressure $P_0 \approx 136$ kbar on the $0^{o}K$ isotherm. In the case of parallel molecules, R = 2.3Å is also the distance between centers-of-mass.

It is interesting to note that $\Delta\mathcal{E}$ reaches a minimum for three molecules at R = 2Å, regardless of orientation, and approaches a constant value as $n \to \infty$. The reason for this behavior is manifested in the nodal and antinodal (bonding) structure of the excited state molecular orbitals. Each of the molecular orbitals for the electronic states has m nodes which oppose bonding, and m' partial bonds between molecules. The number of nodes m is nearly proportional to the number of NO^+ molecules, and m' is nearly proportional to the number of pairs of NO^+ molecules. The ratio r = m/m' is constant for the molecular orbitals in the ground state wave function. On the other hand, r for the excited state π^* molecular orbital, for example, reaches a minimum of 3/2 for $(NO^+)_3$, and is larger for $n \neq 3$. In all cases, the nodal integrity of each NO^+ "molecule" is maintained. The constant value of $\Delta\mathcal{E}$ for large n lies close to the value of $\Delta\mathcal{E}$ = 125 kcal/mole for $(NO^+)_2$. This result suggests that the shifts of excited states for an explosive are primarily functions of the interactions of two or, perhaps, three molecules. This feature implies that extensive calculations of excited states may be performed on only a small number of molecules. These results are expressed even more clearly in Figure 3 where $\Delta\mathcal{E}$, given in kcal per mole of NO^+ molecules, is seen to approach constant values in accordance with Figure 2. Long-range effects are seen to be relatively unimportant for all structures. These effects tend to be greatest for the linear chain since electron mobility among the molecules is largest here.

In accordance with the BO approximation and the corresponding Franck-Condon principle, the excitation energies $\Delta\mathcal{E}$ were computed at fixed nuclear configurations. Unfortunately, limitations within the CNDO/S-CI method preclude the computation of surfaces when the bond distance in NO^+ is substantially greater than its equilibrium value of 1.062Å. We now describe surfaces generated by the LCAO-MO-SCF method.

As mentioned before, the initiation of detonation process involves the breaking of bonds. We are interested in the mechanism which accelerates the rate of bond scission. To this end, the LCAO-MO-SCF method was used to generate cuts out of the total reaction surface of six dimensions for $(NO^+)_2$. One of these cuts, a curve, corresponds to the change in potential energy as N-O bonds are stretched while the other internuclear distances are held fixed. To a good first approximation, the $(NO^+)_2$ system should reflect changes in the N-O bond strength, since Figures 2 and 3 show that this system yields the largest depression of $\Delta\mathcal{E}$ from the single NO^+ molecular value of 173 kcal/mole.

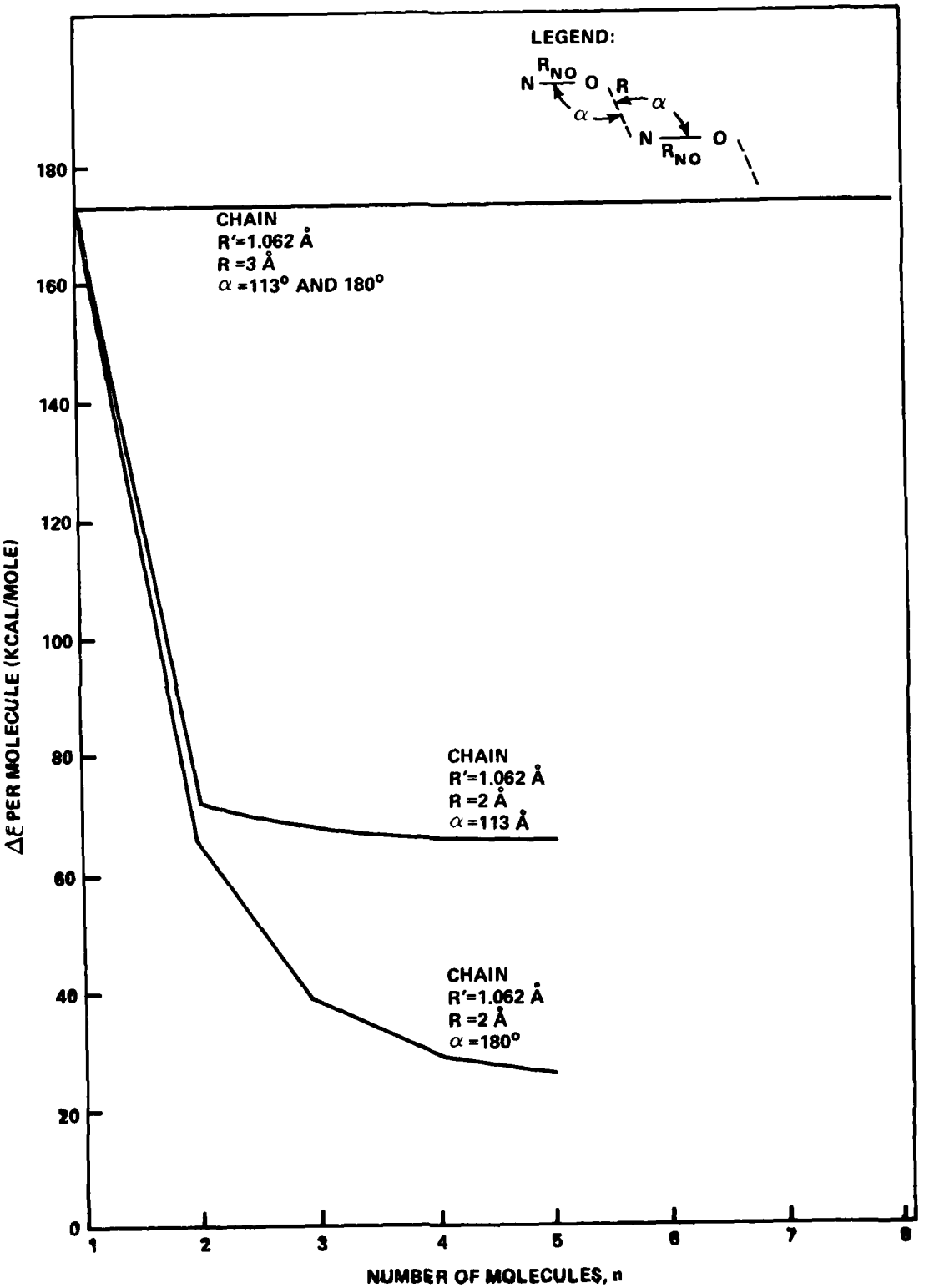

FIGURE 3 EXCITATION ENERGIES PER MOLECULE FOR $(NO^+)_n$

In Figure 4, the ground state potential energy curve $\mathcal{E}_0^{BO}$ (1G) for the isolated molecule is plotted against the N-O bond distance R' expressed in bohr radii (1 bohr = 0.529A). All energies are referred to the minimum at R_{min} = 2.007 bohrs (1.062A). The section of the curve for $R' < R_{min}$ corresponds to the repulsion between atoms. Extension of the curve would show that $\mathcal{E}_0^{BO} \to \infty$. Here, the repulsion of the nuclei dominates $\mathcal{E}_0^{BO}$. The section of the curve for $R' < R'_{min}$ shows a steep rise and an eventual falling off to a limit characteristic of the energy of the atoms N and O^+. The shape of the curve is dictated by the virial theorem relationship of Equation (12) where $E_e = \mathcal{E}_0^{BO}$. The distance from the bottom of the potential well at R_{min} to the plateau for dissociation is approximately 254 kcal/mole. This value pertains to E_{act}^{int} and is similar to the bond dissociation energy, 256 kcal/mole, of CO, which is isoelectronic with NO^+.

The two lowest excited state curves $\mathcal{E}_1^{BO}$(1E) and $\mathcal{E}_2^{BO}$(1E') for NO^+ are also plotted in Figure 4. These curves were obtained from Equation (A7) in Appendix A, using the MO's from the ground state calculation. Since additional computer programming is required, no SCF calculations on the excited states were performed here. An SCF calculation could lower each curve by as much as 30 kcal/mole. It is noted from the shapes of the curves that NO^+ is bound in these excited states. The dissociation limits of $\mathcal{E}_1^{BO}$ and $\mathcal{E}_2^{BO}$ were not computed.

Figure 5 gives the orientations of the two NO^+ molecules in $(NO^+)_2$ for a head-on collision and a broadside collision. These two configurations do not necessarily give the lowest energies for the $(NO^+)_2$ system. They are considered here for direct comparison with the $(NO)_2$ system which is a dimer with the indicated linear configuration (head-on collision) at ambient pressures.[40] This system will be discussed in a future report. The broadside collision provides a direct reaction path for generation of the detonation reaction products N_2 and O_2 in the NO explosive.[41] An LCAO-MO-SCF calculation was performed at each set of values for R and R' where R and R' were chosen in the ranges $1 < R \leq 4$Å (1.9 < R ≤ 7.6 bohrs) and $0.9 \leq R' \leq 1.6$Å (1.7 ≤ R' ≤ 3.0 bohrs). The resulting curves are plotted in Figures 6 and 7.

---

[41] Ramsay, J. B., and Chiles, W. C., "Detonation Characteristics of Liquid Nitric Oxide," in Proceedings of the Sixth Symposium (International) on Detonation, 24 August 1976, pp. 723-728.

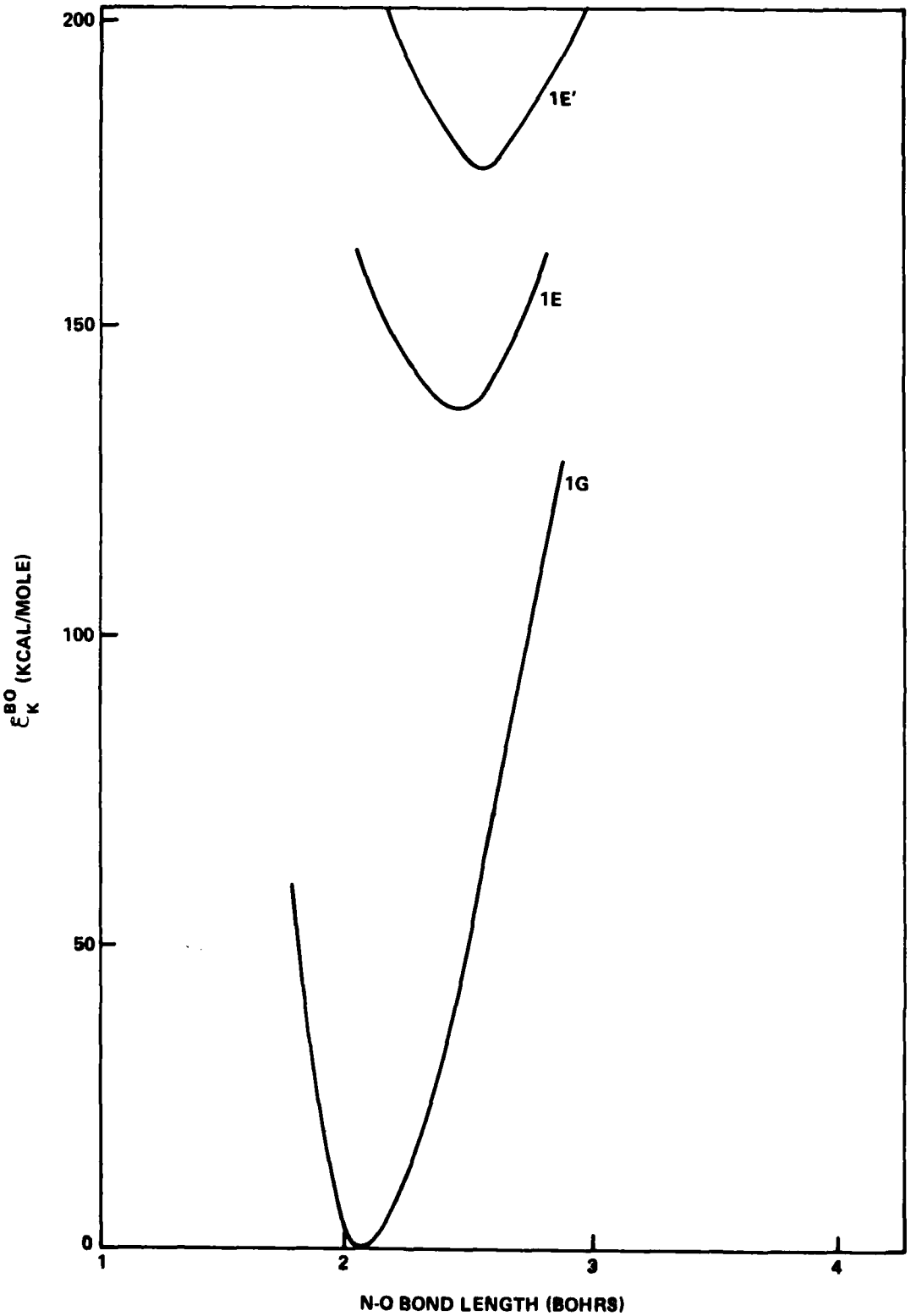

FIGURE 4 ENERGY CURVES FOR NO^+

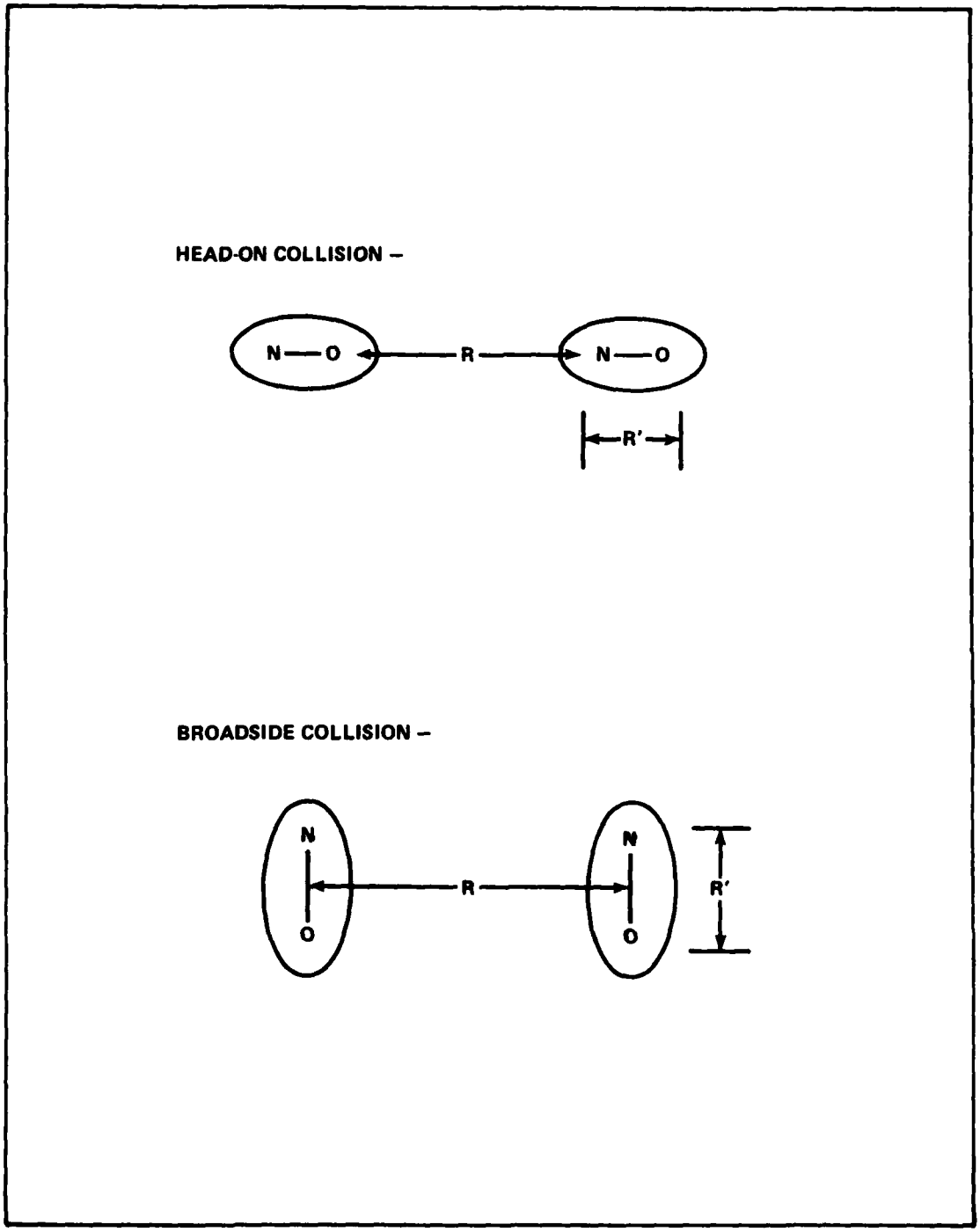

FIGURE 5 TWO INTERACTING NO^+ MOLECULES

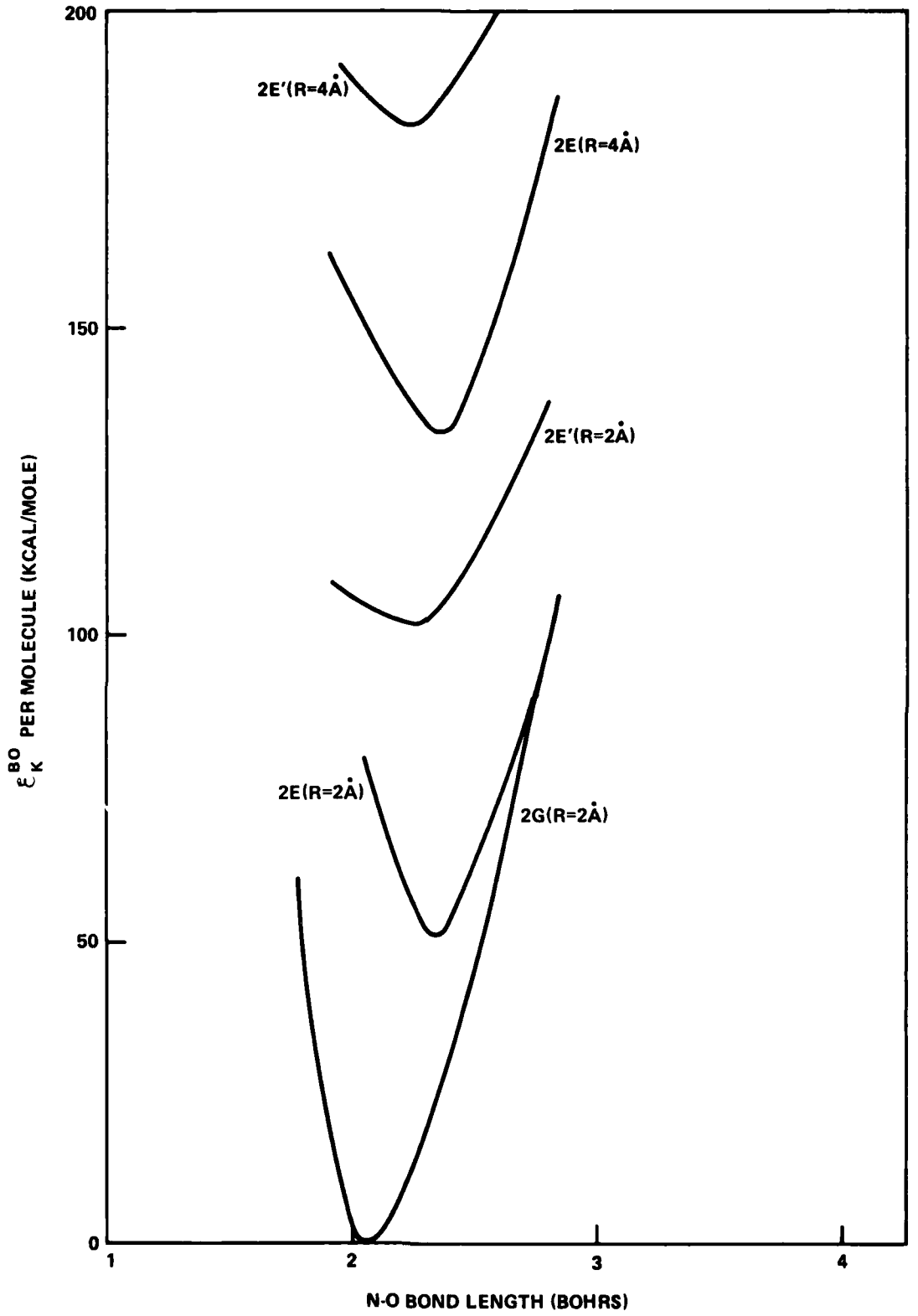

FIGURE 6 ENERGY CURVES FOR BROADSIDE COLLISION

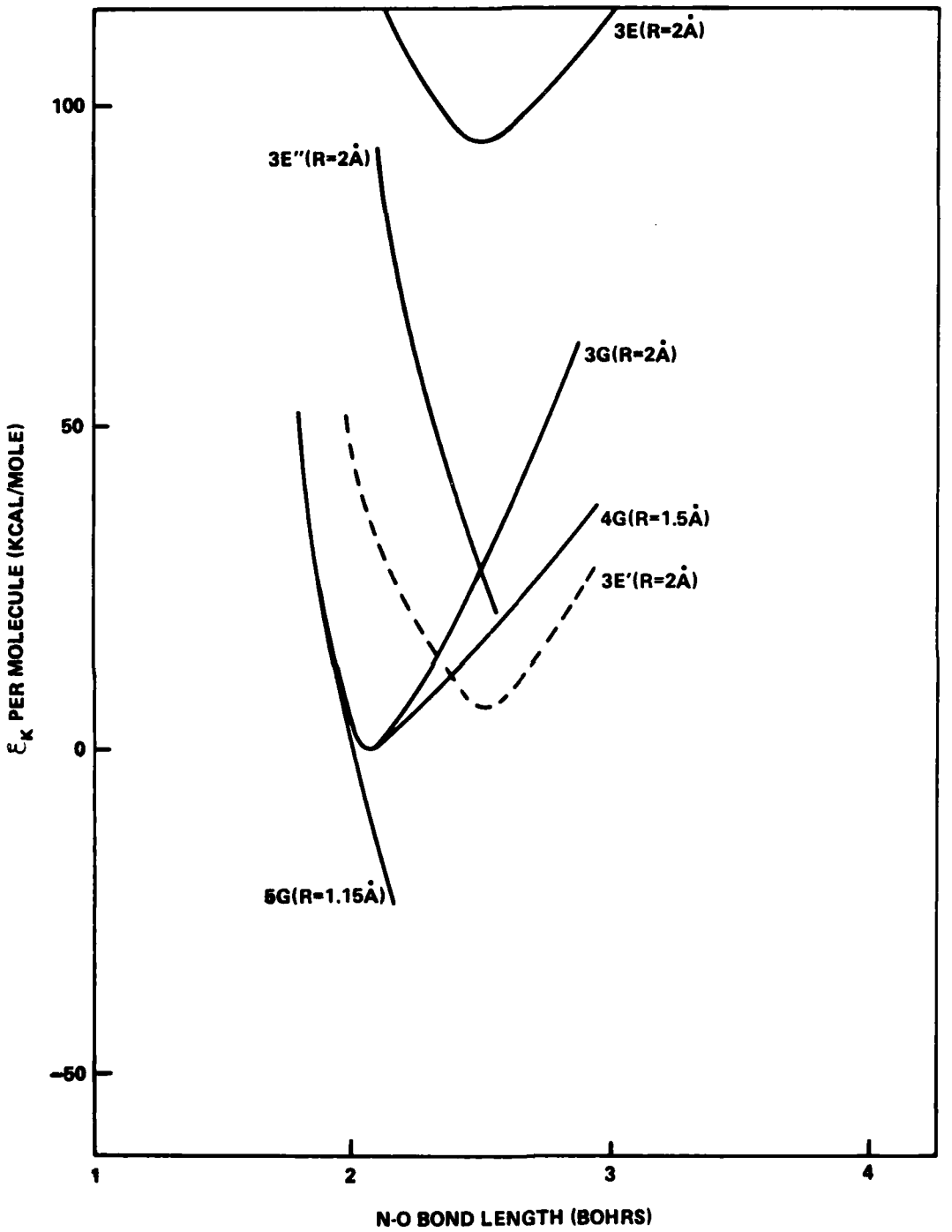

FIGURE 7 ENERGY CURVES FOR HEAD-ON COLLISION

The ground and lowest excited states calculated for the broadside collision are given in Figure 6. These curves were obtained by varying the N-O bond distances together and by the same amount in both molecules, and represent the effective energy per molecule determined by dividing the energy of $(NO^+)_2$ by 2. The ground state curve $\mathcal{E}_0^{BO}(2G)$ is somewhat broader than the 1G curve for NO^+ in Figure 4. Inasmuch as the curves approximate harmonic oscillator potentials, the frequency relationship

$$\nu = \frac{1}{2\pi\mu^{\frac{1}{2}}}\sqrt{\frac{\partial^2 \mathcal{E}_O^{BO}}{\partial R'^2}} \tag{46}$$

may be used to show that the low-lying vibrational energy levels for curve 2G are closer together than those for curve 1G, since

$$\frac{\partial^2 \mathcal{E}_O^{BO}(2G)}{\partial R'^2} < \frac{\partial^2 \mathcal{E}_O^{BO}(1G)}{\partial R'^2} \quad . \tag{47}$$

Consequently, compression shifts infrared (IR) spectra to lower frequencies. If the NO^+ molecules were pushed closer together to a separation of $R \simeq 1.1$Å, bonding would occur between nitrogens to form N_2 and between oxygens to form O_2+2.

Compression also shifts ultraviolet (UV) and visible spectra to lower frequencies. This is seen in Figure 6 by comparing the curves 2E and 2E' at R = 4Å. The allowed vertical transition from 2G to 2E' is shifted by 3.5 ev.

Similar shifts of UV and IR spectra are found for the head-on collision, Figure 7. These curves were obtained by varying the N-O bond distance in <u>one</u> NO^+ molecule, and represent the effective energy per molecule determined as in Figure 6. The curves describe a possible situation where only one N-O bond is breaking during detonation. The ground state curves 4G and 5G indicate substantial broadening at R = 1.5Å and spontaneous decomposition of NO^+ at R = 1.15Å. Calculations for the variation of <u>two</u> NO^+ bonds yield similar results. Curve 3E at R = 2Å represents the same state as curve 1E' in Figure 4 for the isolated molecule, but substantially lower-lying. The dashed curve 3E' at R = 2Å represents a <u>possible</u> position of curve 3E when five NO^+ molecules are interacting in the linear configuration indicated in Figure 2. This curve was not calculated. Curve 3E" at R = 2Å is a dissociative excited state. It intersects the 3G curve at 2.5 bohrs.

Figure 8 describes a <u>possible</u> result of the application of degenerate perturbation theory, using the perturbations of Equation (18) and the matrix element in Equation (42). The dashed portions of the curves were not calculated. The solid portions are the curves 3G and 3E" of Figure 7. Note that a new activation barrier E_{act}^{int} would be created. This barrier would be the one approximated by Equation (43). Calculation would show the size of the gap at

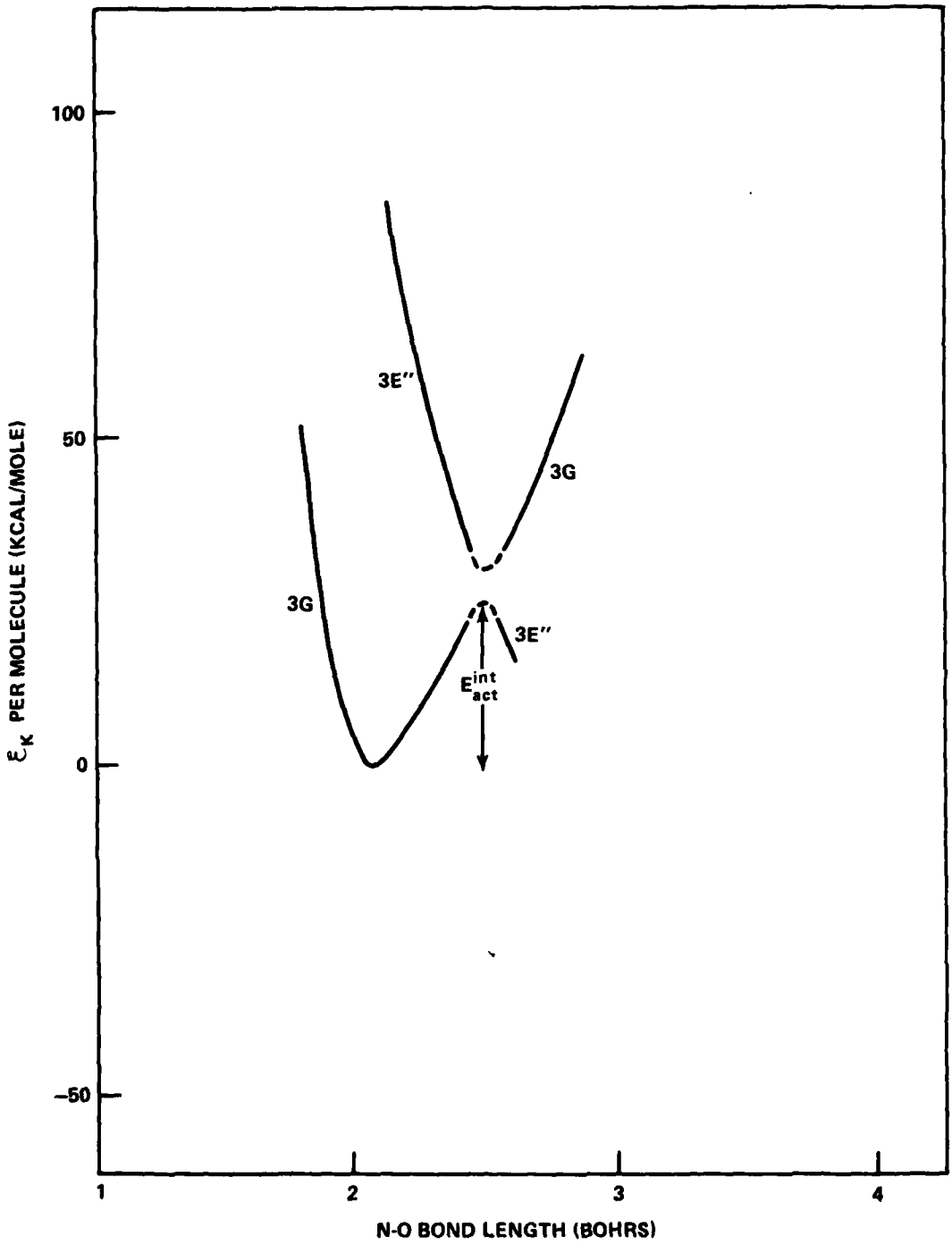

FIGURE 8 ENERGY CURVES RESULTING FROM COUPLING OF ELECTRONIC AND NUCLEAR MOTIONS

the top of the barrier to be $2|\bar{\mathcal{E}}_{12}|$. As $|\bar{\mathcal{E}}_{12}|$ increases, so does the probability P', Equation (39), that the reaction takes place on the lower curve. Thus, the N-O bond in NO^+ will break more easily when $|\bar{\mathcal{E}}_{12}|$ is sufficiently large and E_{act}^{int} is sufficiently small. The quantity $\bar{\mathcal{E}}_{12}$ in Equation (42) will be calculated and the results presented in a future report.

The curves 3G and 3E" are electronic states of different symmetry, and are designated as $^1\Sigma^+$ and $^3\pi$, respectively. The designation $^1\Sigma^+$ describes a spin singlet state, $S^2\Psi_0 = 0$, which has a projection of zero electronic orbital angular momentum along the bond axis, $L_z\Psi_0 = 0$. The designation $^3\pi$ describes a triplet state, $S^2\Psi_1 = 2\hbar^2\Psi_1$, which satisfies $L_z\Psi_1 = \pm\hbar\Psi_1$. For these states, $\langle\Psi_0|H_e|\Psi_1\rangle = 0$, so that the conditions in Equation (29) are satisfied at the intersection.

Figure 9 contains the repulsion energies for the $(NO^+)_2$ system in the head-on and broadside collisions. The estimated pressures along the 0°K isotherm are indicated at various intermolecular separations. The N-O bonds are fixed at $R'_{min} = 1.062\text{Å}$ for NO^+. These pressures were calculated from

$$P_o = -\frac{d\bar{\mathcal{E}}_0}{dv} \simeq -\frac{1}{3R_{CM}^2}\frac{\partial\bar{\mathcal{E}}_0}{\partial R} \quad , \tag{48}$$

where R_{CM} is the distance between the nuclear centers-of-mass of the NO^+ molecules. $\bar{\mathcal{E}}_0$ is the effective energy per molecule, and v is assumed to be the average volume per molecule, $v = R_{CM}^3$, which pertains to a simple cubic lattice. The derivatives $\partial\bar{\mathcal{E}}_0/\partial R$ were evaluated numerically, using a three-point, divided-difference formula. The two curves do not represent the same compression since v refers to the separations of the nuclear centers-of-mass. For example, $R_{CM} = R = 2\text{Å}$ for the broadside collision, and $R_{CM} = 3.062\text{Å}$ at $R = 2\text{Å}$ for the head-on collision.

It was mentioned in the previous paragraph that the derivative in Equation (48) was calculated numerically. This procedure is considerably more acurate than the evaluation of $\partial\bar{\mathcal{E}}_0/\partial R$ from the virial theorem, Equation (12). Although $\bar{K}_e$ is calculated in the LCAO-MO-SCF method, it is not determined accurately enough relative to $\bar{\mathcal{E}}_0$ and $\partial\bar{\mathcal{E}}_0/\partial R$, since Equation (12) results from a variational calculation on all of the parameters contained in the wave function Ψ_0. As discussed in Appendix A, the LCAO-MO-SCF method requires variation of only linear expansion coefficients in the MO's. Consequently, Equation (12) applies to an exact Hartree-Fock calculation, and only approximately to the calculations performed here.

The pressures shown in Figure 9 are upper limits to actual values of P_0 for $(NO^+)_2$. This is due to the nature of the methods used here and of the exact Hartree-Fock methods (HFM). Only at very high compressions, where the nuclear repulsion energy dominates $\mathcal{E}_0$, are the values for P_0 accurately determined. At low compressions ($R > 2.5\text{Å}$), configuration interaction (CI) methods which introduce electron correlation are essential. In fact, since Hartree-Fock theory does not introduce correlation between electrons of the opposite spin, it cannot produce a minimum in the interaction energy corresponding to the van der Waals forces between molecules. The most important term due to correlation is the dispersion energy E_d, defined by[23]

$$E_d = E_{int} - \mathcal{E}_{HF}\left[(NO^+)_2\right] + 2\mathcal{E}_{HF}\left[NO^+\right] \quad , \tag{49}$$

where E_{int} is the exact interaction energy obtained from the eigenvalue E in Equation (24), $\mathcal{E}_{HF}[(NO^+)_2]$ is the Hartree-Fock energy of the $(NO^+)_2$ system, and $\mathcal{E}_{HF}(NO^+)$ is the Hartree-Fock energy of the isolated NO^+ molecule. In the LCAO-MO-SCF method, it is assumed that the errors generated by not performing exact Hartree-Fock calculations are similar in NO^+ and $(NO^+)_2$ so that substantial cancellation occurs in Equation (49). Then, the difference in the Hartree-Fock energies yields the classical Coulomb interaction energy, the first-order exchange, the induction energies, some of the second-order exchange including the charge transfer part, and some higher-order terms. Reference 23 may be consulted for a discussion of these contributions. Since E_d is a negative quantity (for molecular attraction) which varies approximately as $-R^{-6}$, the derivative of Equation (49) shows that the P_0 values in Figure 9 are too high by $(1/3R_{CM}^2)(\partial E_d/\partial R)$.

The neglect of electron correlation also leads to errors in the relative placements of the ground and excited state curves in Figures 4-8. The results of the CNDO/S-CI calculations show that the introduction of electron correlation can reduce the separation of the curves by as much as 45 kcal/mole for $(NO^+)_2$ or 23 kcal/mole for NO^+. Consequently, the estimated barrier and E_{act}^{int} in Figure 8 will be smaller.

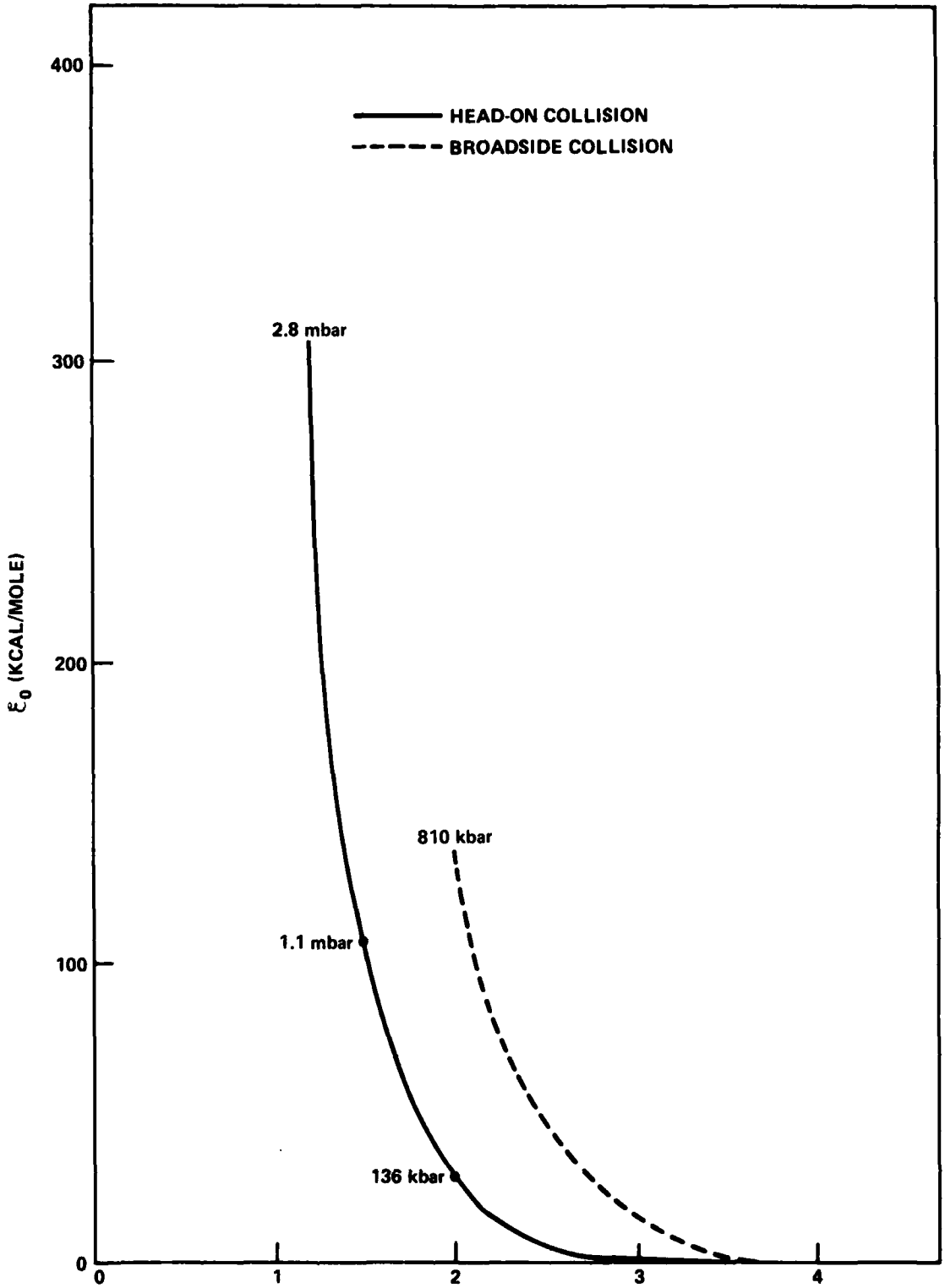

FIGURE 9 REPULSION ENERGIES AND P_0 VALUES FOR $(NO^+)_2$

SUMMARY AND FUTURE WORK TO BE PERFORMED

The theoretical basis for an analysis of ground and excited state potential energy surfaces has been presented. The behavior of the ground and excited state surfaces of molecular systems under compression was examined within the framework of the Born-Oppenheimer (BO) approximation, and from the standpoint of intersections of the surfaces which result in a breakdown of the BO approximation.

An application of the theory was made to the $(NO^+)_n$ system. Excitation energies $\Delta\varepsilon$ for the first excited state of linear $(NO^+)_n$ decreased from $\Delta\varepsilon$ =173 kcal/mole for n = 1 to 125 kcal/mole for n = 2, and to $\Delta\varepsilon$ = 100 kcal/mole for n = 3. The molecules were separated by 3Å between their centers-of-mass. For $3 < n < 6$, $\Delta\varepsilon$ increased and approached a plateau at ~120 kcal/mole. This plateau is close to the value of $\Delta\varepsilon$ for $(NO^+)_2$ which suggests that the detailed study of excitation energies and activation energies can be carried out on just two or three interacting molecules. Minima were reached at n = 3 for other orientations of the NO^+ molecules. Recent results for two interacting nitromethane molecules indicate that a similar precipitous drop in $\Delta\varepsilon$ occurs. Calculations on nitromethane are continuing.

It was seen that the ground state curves for the N-O bond stretch in $(NO^+)_2$ describe a bound system for intermolecular distances greater than about 1.15Å. At distances less than 2Å, the curves are broadened considerably, indicating a weakened bond. At the distance of 1.15Å, the curve collapses, suggesting spontaneous decomposition of NO^+ at high compression. A broadening of a ground state curve indicates that the vibrational spectra are shifted to lower frequencies. The UV spectra are also shifted to lower frequencies.

Intersections of the ground and excited state curves are found for $(NO^+)_2$ when the centers-of-mass of the molecules are separated by 3Å or less. These intersections generate new barriers to bond scission which are substantially less than the barrier height of ~250 kcal/mole in the gas phase.

These calculations on $(NO^+)_n$ constitute the first stage in a complete series of calculations which will also involve the use of perturbation theory to lift the degeneracies (intersections). Some additional mathematical details are to be worked out in the perturbation analysis. For example, the wave equations for the n-molecule system must be derived. A new stage of calculations involving these wave equations will complete the description of the kinetics of the bond scission process, and will be presented in a future report. The calculations in the present report will be refined further by complete Hartree-Fock and CI calculations on the excited states. The sequence of calculations on $(NO^+)_n$ will serve as a guide for those to be done on $(NO)_n$ and nitromethane.

REFERENCES

1. Kamlet, M. J., "The Relationship of Impact Sensitivity with Structure of Organic High Explosives. I. Polynitroaliphatic Explosives," in Proceedings of the Sixth Symposium (International) on Detonation, 24 August 1976, pp. 312-322.

2. Bowden, F. P., and Yoffe, A. D., Initiation and Growth of Explosions in Liquids and Solids, (Cambridge University Press, 1952).

3. Price, D., "Shock Sensitivity, A Property of Many Aspects," in Proceedings of the Fifth Symposium (International) on Detonation, 18 August 1970, pp. 207-217.

4. Pastine, D. J., Edwards, D. J., Jones, H. D., Richmond, C. T., and Kim, K., "Some New Concepts Relating to the Initiation and Failure of Detonable Explosives," in Timmerhaus, K. D., and Barber, M. S., eds., High Pressure Science and Technology, Vol. 2, (New York: Plenum Publishing Corp., 1979), pp. 364-382.

5. Pastine, D. J., and Bernecker, R. R., "P,V,E,T Equation of State for 1,3,5-triamino-2,4,6-trinitrobenzene," Journal of Applied Physics, Vol. 45, No. 10, 1974, p. 4458.

6. Campbell, A. W., Davis, W. C., and Travis, J. R., "Shock Initiation of Detonation in Liquid Explosives," Physics of Fluids, Vol. 4, 1961, p. 498.

7. Bardo, R. D., Hall, T. N., and Kamlet, M. J., "The Volume of Activation in the Shock Initiation of Explosives," Combustion and Flame, Vol. 35, 1979, p. 259.

8. Haskins, P. J., "Electronic Structure of Some Explosives and Its Relationship to Sensitivity," Research in Primary Explosives-ERDE 1975, Presentation No. 6, 1975.

9. Delpuech, A., and Cherville, J., "Relation entre la Structure et la Sensibilité au Choc des Explosifs Secondaires Nitrés-Critére Moléculaire de Sensibilité. I. Cas des Nitroaromatiques et des Nitramines," Propellants and Explosives, Vol. 3, 1978, p. 169.

10. Bardo, R. D., and Wolfsberg, M., "The Wave Equation of a Nonlinear Triatomic Molecule and the Adiabatic Correction to the Born-Oppenheimer Approximation," Journal of Chemical Physics, Vol. 67, No. 2, 1977, p. 593.

11. Hardesty, D. R., "An Investigation of the Shock Initiation of Liquid Nitromethane," Combustion and Flame, Vol. 27, 1976, p. 229.

12. U. S. Army Materiel Command, Engineering Design Handbook, Principles of Explosive Behavior, 1972, Chapter 11, pp. 1-32.

13. Bridgman, P. W., "Effects of High Shearing Stress Combined with High Hydrostatic Pressure," Physical Review, Vol. 48, 1935, p. 825.

14. Teller, E., "On the Speed of Reactions at High Pressures," Journal of Chemical Physics, Vol. 36, No. 4, 1962, p. 901.

15. Johnson, Q., Mitchell, A., Keeler, R. N., and Evans, L., "X-ray Diffraction during Shock Wave Compression," Physical Review Letters, Vol. 25, 1970, p. 1099. In this paper, the results of the X-ray analysis of crystalline LiF demonstrate that the uniaxially strained crystal produced by a 130 kbar shock relaxes to an isotropic structure in a time which is short compared to 20 nanoseconds.

16. Laidler, K. J., Chemical Kinetics (New York: McGraw-Hill Book Co., Inc., 1965), pp. 72-112.

17. Slater, J. C., Quantum Theory of Atomic Structure, Volume II, (New York: McGraw-Hill Book Co., Inc., 1960), pp. 1-30.

18. Dunning, Jr., T. H., Cartwright, D. C., Hunt, W. J., Hay, P. J., and Bobrowicz, F. W., "Generalized Valence Bond Calculations on the Ground State ($X^1\Sigma^+g$) of Nitrogen," Journal of Chemical Physics, Vol. 64, No. 11, 1976, p. 4755, and other references cited therein.

19. Bethe, H. A., "Nuclear Many-Body Problem," Physical Review, Vol. 103, No. 5, 1956, p. 1353.

20. Jacobs, S. J., "On the Equation of State for Detonation Products at High Density," in Twelfth Symposium (International) on Combustion, 1969, pp. 501-511.

21. Hirschfelder, J. O. Curtiss, C. F., and Bird, R. B., Molecular Theory of Gases and Liquids,(New York: John Wiley & Sons, Inc., 1954), pp. 134-135.

22. Slater, J. C., Quantum Theory of Molecules and Solids, Volume I, (New York: McGraw-Hill Book Co., Inc., 1963), pp. 29-40.

23. Amos, A. T., and Crispin, R. J., "Calculations of Intermolecular Interaction Energies," in Eyring, H., and Henderson, D., eds., Theoretical Chemistry, Advances and Perspectives, Vol. 2, (New York: Academic Press, 1976), pp. 33-35.

24. Feynman, R. P., "Forces in Molecules," Physical Review, Vol. 56, 1939, p. 340.

25. Ross, M., and Shishkevish, C., "Molecular and Metallic Hydrogen," R-2056-ARPA, 1977.

26. Blais, N. C., and Bunker, D. L., "Monte Carlo Calculations. II. The Reactions of Alkali Atoms with Methyl Iodide," Journal of Chemical Physics, Vol. 37, No. 11, 1962, p. 2713. See also Karo, A. M., and Hardy, J. R., "Molecular Dynamics of Shock-Initiated Detonations," International Journal of Quantum Chemistry, Vol. 12, Suppl. 1, 1977, p. 333.

27. Bardo, R. D., and Wolfsberg, M., "A Theoretical Calculation of the Equilibrium Constant for the Isotopic Exchange Reaction between H_2O and HD," Journal of Physical Chemistry, Vol. 80, No. 10, 1976, p. 1068. It was shown in this paper that the adiabatic correction leads to equilibrium constants which differ from the experimental ones by less than the experimental error.

28. Teller, E., "The Crossing of Potential Surfaces," Journal of Physical Chemistry, Vol. 41, No. 1, 1937, p. 109.

29. Carrington, T., "The Geometry of Intersecting Potential Surfaces," Accounts of Chemical Research , Vol. 7, 1974, p. 20.

30. Jortner, J., Rice, S. A., and Hochstrasser, R. M., "Radiationless Transitions in Photochemistry," in Noyes, W. A. et al., eds., Advances in Photochemistry, Vol. 7, (New York: Wiley, 1969), pp. 149-309.

31. Longuet-Higgins, H. C., "The Intersection of Potential Energy Surfaces in Polyatomic Molecules," Proceedings of the Royal Society, London, Vol. A344, 1975, p. 147.

32. von Neumann, J., and Wigner, E., "Uber das Verhalten von Eigenwerten bei adiabatischen Prozessen," Zeitschrift für Physik, Vol. 30, 1929, p. 467.

33. Hatton, G. J., "The Noncrossing Rule and Spurious Avoided Crossings," Physical Review A, Vol. 14, No. 3, 1976. p. 901.

34. Zener, C., "Non-Adiabatic Crossing of Energy Levels," Proceedings of the Royal Society of London,Ser. A, Vol. 137, 1932, p. 696.

35. Landau, L. D., and Lifshitz, E. M., Quantum Mechanics, 2nd Edition, (Reading, Mass.: Addison-Wesley Publishing Co., Inc., 1965), pp. 322-330.

36. Stückelberg, E. C. G., "Theorie der Unelastischen Stösse Zwischen Atomen," Helvetica Physica Acta, Vol. 5, 1932, p. 369.

37. Eyring, H., Walter, J. and Kimball, G. E., Quantum Chemistry (New York: John Wiley & Sons, Inc., 1944), pp. 299-331.

38. Roothaan, C. C. J., "New Developments in Molecular Orbital Theory," Reviews of Modern Physics, Vol. 23, No. 2, 1951, p. 69.

39. Del Bene, J., and Jaffe, H. H., "Use of the CNDO Method in Spectroscopy. I. Benzene, Pyridine, and the Diazines," Journal of Chemical Physics, Vol 48, No. 4, 1968, p. 1807, and references cited therein.

40. Ohlsen, J. R., and-Laane, J., "Characterization of the Asymmetric Nitric Oxide Dimer O = N - O = N by Resonance Raman and Infrared Spectroscopy," Journal of American Physical Society, Vol, 100, No. 22, 1978, p. 6948.

41. Ramsay, J. B., and Chiles, W. C., "Detonation Characteristics of Liquid Nitric Oxide," in Proceedings of the Sixth Symposium (International) on Detonation, 24 August 1976, pp. 723-728.

Appendix A

DESCRIPTION OF COMPUTATIONAL METHODS

The treatment of the electron many-body problem in the solution of Equation (24) is usually made by the method of configuration interaction (CI). Here, the eigenfunction Φ_K is expressed as a linear combination of Slater determinants Ψ_I,

$$\Phi_K = \sum_{I=0}^{\infty} C_{KI} \Psi_I \quad . \tag{A-1}$$

Each determinant Ψ_I of dimension N, the number of electrons, is constructed from N spin-orbitals selected from a complete set of an infinite number of orthonormal spin-orbitals, $\{u_k\}$. Each spin-orbital $u_k = \rho_{k\alpha}$ is a function of the coordinates of a single electron so that Ψ_I can be expressed as

$$\Psi_I = A\left\{u_1(1)u_2(2) \ \ldots \ u_N(N)\right\} \quad , \tag{A-2}$$

where A is an antisymmetrizer operator. The complete set of spin-orbitals is generated from a Hartree-Fock calculation which minimizes the energy given by

$$\mathcal{E}_0 = \langle \Psi_0 | H_e | \Psi_0 \rangle \quad , \tag{A-3}$$

subject to constraints on the orthonormality of the spatial parts ρ_k of the spin-orbitals. The solution of the simultaneous equations

$$\sum_J \left\{\Psi_I | H_e | \Psi_J - E_K \delta_{IJ}\right\} C_{KJ} = 0 \tag{A-4}$$

yields the manifold of electronic ground and excited states.

The solution of Equation (A-3) is made tractible by the careful selection of combinations of spin-orbitals which provide the most rapid convergence in Equation (A-1). The success of this procedure depends in large part on the solution of Equation (A-3), which is made tractible by a method devised by Roothaan in Reference 38. This method is called the linear combination of atomic orbitals (LCAO) molecular orbital (MO) self-consistent field (SCF) method, the LCAO-MO-SCF method. Here, each MO u_k is expressed in terms of the finite set of AO's $\{g_i\}$,

$$u_k = \sum_i c_{ki} g_i \quad . \tag{A-5}$$

A careful selection of a basis set of AO's $\{g_i\}$ often permits the calculation of the ground state energy $\mathcal{E}_o$ which is 95-99% of the experimental energy E_o at certain nuclear configurations, including the equilibrium positions of the nuclei. As a consequence, Equation (A-1) reduces to $\Phi_0 \simeq \Psi_0$ for a closed-shell molecular ground state. In the case of an excited state corresponding to an open-shell electronic configuration, Φ_K is often expressed in terms of two or more determinants. The quantity $E_K - \mathcal{E}_K$ is often referred to as the correlation energy. This energy reflects the detailed interactions between electrons which were ignored in the solution of Equation (A-3).

The coefficients c_{ki} in Equation (A-5) are obtained by solving the pseudo-eigenvalue SCF equations

$$\hat{F}\,\hat{c} = \hat{e}\,\hat{S}\,\hat{c} \tag{A-6}$$

in conjunction with the minimization of the energy

$$\mathcal{E}_K = \hat{H}^{\dagger}\hat{D}_T + \tfrac{1}{2}\hat{D}_T^{\dagger}\hat{P} - \tfrac{1}{2}\hat{D}_O^{\dagger}\hat{Q} \quad . \tag{A-7}$$

The solution of these equations constitutes the variational method of the SCF approximation. In these equations $\hat{F}$, $\hat{H}$, $\hat{P}$, and $\hat{Q}$ are matrices with matrix elements containing kinetic energy, electron-nuclear attraction, and Coulomb and exchange electron-repulsion integrals over the AO's. $\hat{D}_T$ and $\hat{D}_O$ are density matrices containing the coefficients c_{ki}. S is an overlap matrix, and $\hat{\epsilon}$ is a diagonal matrix which contains the orbital energies. Equations (A-6) and (A-7) frequently provide accurate descriptions of quantum mechanical systems, and can usually be solved at relatively low cost. Great strides have been made toward large reductions in the cost of these calculations on large molecular systems.

Equation (A-7) describes the averaged interactions of electrons. As a consequence, it may yield surfaces which have incorrect shapes. This problem will arise when the correlation energy varies greatly with nuclear configuration. Therefore, a compromise must be struck between the solution of the higher cost, accurate CI methods and the lower cost, less accurate SCF methods. The trick is to reduce the number of basis functions in Equation (A-1) to a point where CI methods can be used in large molecular systems. Then, a variational calculation on the coefficients D_{KJ} in a limited basis set yields a finite set of equations, Equation (A-4), which can be solved. Perhaps the most promising approach introduced so far is the CI-related method called the generalized valence bond (GVB) method.[18]

All of the methods described above are ab initio methods. They require the processing of $M^4/8$ two-electron integrals where M is the number of AO's. A great deal of work has gone into devising semiempirical techniques which can be used for large molecules at low cost. The one which is most widely used is the complete neglect of differential overlap (CNDO) method. Here, a large number of electron repulsion integrals are eliminated by virtue of their small values as dictated by the magnitude ofthe differential overlap of AO's occurring in them. Also, only the valence orbitals are treated explicitly in the SCF procedure while the core shell contributions are fixed and determined by parameters defined in terms of experimental ionization potentials. Parameterizations in the method have been refined to the point where reliable results can be obtained for a wide variety of molecular properties. A method which yields reliable electron excitation energies for many systems by combining the best features of the CNDO and CI techniques is called the CNDO/S-CI method.[39] It employs equations similar to Equations (A-1) - (A-7). This technique is of particular value for the present calculations.

DISTRIBUTION

	Copies
Director Headquarters Naval Material Command Attn: MAT-08T2 (Tibor Horwath) Washington, DC 20360	1
Director Defense Documentation Center Cameron Station Alexandria, VA 22314	12
Director of Navy Laboratories Attn: J. H. Probus Crystal Plaza 5 Arlington, VA 20360	1
Commander Naval Sea Systems Command Attn: SEA-03B	1
SEA-62R (W. W. Blaine)	1
SEA-64E (R. Beauregard)	1
Technical Library Arlington, VA 20362	2
Commander Naval Air Systems Command Attn: AIR-350	1
AIR-350D (H. Benefiel)	1
AIR-350F (R. J. Wasneski)	1
AIR-440 (H. Mueller)	1
AIR-950D (Technical Library) Department of the Navy Arlington, VA 20360	1

DISTRIBUTION (Cont.)

	Copies
Chief of Naval Research	
Office of Naval Research	
Attn: ONR-102 (J. Smith)	1
ONR-473 (R. S. Miller)	1
ONR-420 (T. Berlincourt)	1
ONR-421 (W. Condell)	1
ONR-421 (R. Junker)	1
ONR-465 (E. Salkovitz)	1
ONR-473 (J. Satkowski)	1
Technical Library	1
Arlington, VA 22217	
Commanding Officer	
Naval Ordnance Station	
Attn: Research and Development Department	1
Technical Library	1
Indian Head, MD 20640	
Commander	
Naval Weapons Center	
Attn: A. Addison	1
T. Joyner	1
A. B. Amster	1
Technical Library	1
China Lake, CA 93555	
Commander	
Naval Research Laboratory	
Attn: J. Schnur	1
W. Faust	1
H. Carhart	1
W. Moniz	1
Technical Library	1
Washington, DC 20375	
Pentagon	
OSD (DDRE)	
Attn: G. Gamota	1
A. Adicoff	1
Washington, DC 20301	
Pentagon	
ODDRE	
Attn: R. Thorkildsen	1
Washington, DC 20301	

DISTRIBUTION (Cont.)

	Copies
Commanding Officer U. S. Army Armament Research and Development Command	
Attn: R. Walker	1
N. Slagg	1
O. Sandus	1
J. Alster	1
C. Capellos	1
F. Owens	1
Technical Library	1
Dover, NJ 07801	
Commanding Officer Army Ballistics Research Laboratory	
Attn: R. Frey	1
P. Howe	1
Technical Library	1
Aberdeen, MD 21005	
Director Air Force Office of Scientific Research	
Attn: Col. H. Bryan	1
L. Kravitz	1
Library	1
Bolling Air Force Base Washington, DC 20332	
Commander Air Force Armament Development and Test Center Attn: M. Zimmer Eglin Air Force Base, FL 32542	1
U. S. Department of the Interior Bureau of Mines Attn: R. Watson 4800 Forbes Avenue Pittsburgh, PA 15213	1

DISTRIBUTION (Cont.)

	Copies
Director Lawrence Livermore Laboratory Attn: N. Keeler	1
B. Hayes	1
E. Lee	1
F. Ree	1
M. Finger	1
R. McGuire	1
C. Tarver	1
A. Karo	1
F. Walker	1
M. Ross	1
W. Nellis	1
Technical Library P. O. Box 808 Livermore, CA 94550	1
Director Los Alamos Scientific Laboratory Attn: W. Davis	1
R. Rogers	1
W. Fickett	1
C. Mader	1
J. Bdzil	1
J. Wackerle	1
J. Shaner	1
G. Hughes	1
M. Fowler	1
Technical Library P. O. Box 1663 Los Alamos, NM 87545	1
Director Sandia Laboratories Attn: D. Hayes	1
J. Kennedy	1
J. Nunziato	1
L. Davison	1
R. Graham	1
Technical Library P. O. Box 5800 Albuquerque, NM 87115	1
SRI International Attn: M. Cowperthwaite 333 Ravenswood Avenue Menlo Park, CA 94025	1

DISTRIBUTION (Cont.)

	Copies
University of California, Irvine Department of Chemistry Attn: Professor M. Wolfsberg Irvine, CA 92717	1
Washington State University Department of Physics Attn: Professor G. Duvall Pullman, WA 99163	1
University of Utah Department of Chemistry Attn: Professor H. Eyring Dean of Graduate School Salt Lake City, UT 84112	1
Director Johns-Hopkins Applied Physics Laboratory Attn: S. Koslov J. Kincaid Technical Library Johns-Hopkins Road Laurel, MD 20810	1 1 1
Library of Congress Attn: Gift and Exchange Division Washington, DC 20540	4

NDW-NSWC(W)-5605/1 (Rev. 5-78)

TO AID IN UPDATING THE DISTRIBUTION LIST FOR NAVAL SURFACE WEAPONS CENTER, WHITE OAK TECHNICAL REPORTS PLEASE COMPLETE THE FORM BELOW:

TO ALL HOLDERS OF NSWC TR 79-175
by Richard D. Bardo
DO NOT RETURN THIS FORM IF ALL INFORMATION IS CURRENT

A. FACILITY NAME AND ADDRESS *(OLD) (Show Zip Code)*

NEW ADDRESS *(Show Zip Code)*

B. ATTENTION LINE ADDRESSES:

C.

☐ REMOVE THIS FACILITY FROM THE DISTRIBUTION LIST FOR TECHNICAL REPORTS ON THIS SUBJECT.

D.
NUMBER OF COPIES DESIRED _____

GPO 920-784

DEPARTMENT OF THE NAVY
NAVAL SURFACE WEAPONS CENTER
WHITE OAK, SILVER SPRING, MD. 20910

OFFICIAL BUSINESS
PENALTY FOR PRIVATE USE, $300

POSTAGE AND FEES PAID
DEPARTMENT OF THE NAVY
DOD 316

COMMANDER
NAVAL SURFACE WEAPONS CENTER
WHITE OAK, SILVER SPRING, MARYLAND 20910

ATTENTION: CODE R 13